

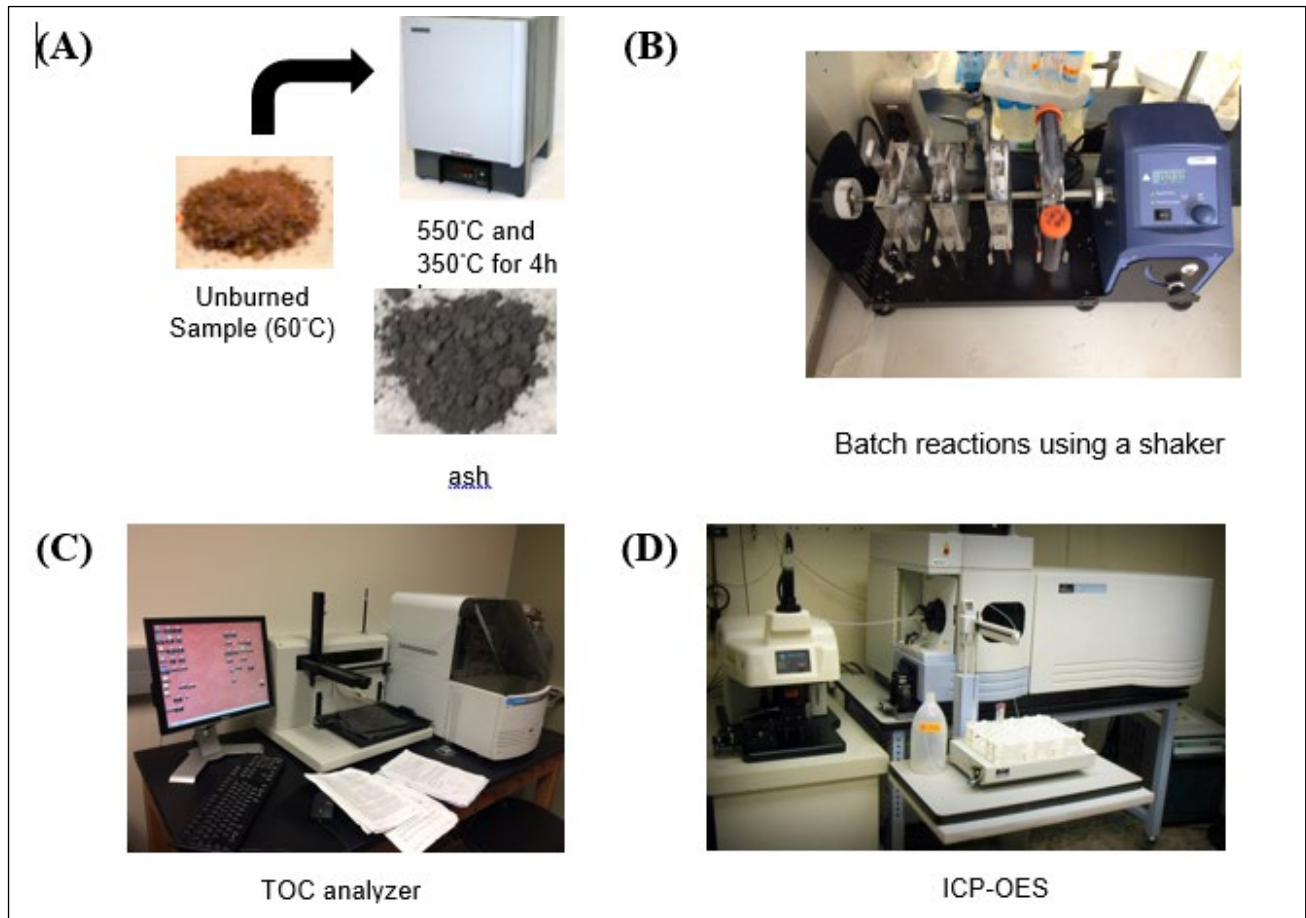
November 2018

## EFFECT OF WILDFIRE ASH ON WATER QUALITY

---

### WRRI Technical Completion Report No. 379

José M. Cerrato  
Asifur Rahman



Materials and methods used for the analysis (page 4)

New Mexico Water Resources Research Institute  
New Mexico State University  
MSC 3167, P.O. Box 30001  
Las Cruces, New Mexico 88003-0001  
(575) 646-4337 email: nmwrri@nmsu.edu





# EFFECT OF WILDFIRE ASH ON WATER QUALITY

By

José M. Cerrato, Assistant Professor

Asifur Rahman, Research Assistant

Department of Civil Engineering

University of New Mexico

TECHNICAL COMPLETION REPORT

Account Number EQ01902

November 2018

New Mexico Water Resources Research Institute

in cooperation with the

Department of Civil Engineering

University of New Mexico

The research on which this report is based was financed in part by the U.S. Department of the Interior,  
Geological Survey, through the New Mexico Water Resources Research Institute Grant  
#G16AP00072

## DISCLAIMER

The purpose of the New Mexico Water Resources Research Institute (NM WRRI) technical reports is to provide a timely outlet for research results obtained on projects supported in whole or in part by the institute. Through these reports the NM WRRI promotes the free exchange of information and ideas and hopes to stimulate thoughtful discussions and actions that may lead to resolution of water problems. The NM WRRI, through peer review of draft reports, attempts to substantiate the accuracy of information contained within its reports, but the views expressed are those of the authors and do not necessarily reflect those of the NM WRRI or its reviewers. Contents of this publication do not necessarily reflect the views and policies of the Department of the Interior, nor does the mention of trade names or commercial products constitute their endorsement by the United States government.

## ACKNOWLEDGEMENTS

Thanks to Dr. Robert Parmenter for scientific advice and support for this study. Funding for this research was provided by the New Mexico Water Resources Research Institute. Additional support was also provided by the Oak Ridge Associated Universities (ORAU) Program and the National Science Foundation under New Mexico EPSCoR (Grant Number #IIA-1301346). Any opinions, findings, and conclusions or recommendations expressed in this publication are those of the author(s) and do not necessarily reflect the views of the Agencies.

## ABSTRACT

We investigated interfacial processes affecting metal mobility in wood ash burned under laboratory-controlled conditions using aqueous chemistry, microscopy, and spectroscopy analyses. Wood was collected from the Valles Caldera National Preserve in New Mexico, which has experienced two wildfires since 2011 that have caused devastating effects. Wood samples (e.g., Ponderosa Pine, Quaking Aspen, and Colorado Blue Spruce) collected from this site were exposed to temperatures of 60°C, 350°C and 550°C. Pine ashes burned at 350°C and 550°C were associated with high concentrations of metals (i.e., Cu, Cr, Si, Ni, Fe, K and Mg). Pine ash burned at 350°C had the highest content of Cu ( $4997 \pm 262 \text{ mg kg}^{-1}$ ), Cr ( $543 \pm 124 \text{ mg kg}^{-1}$ ), and labile dissolved organic carbon (DOC,  $11.3 \pm 0.28 \text{ mg L}^{-1}$ ). Metal sorption experiments were conducted by reacting 350°C Pine ash separately with 10µM solutions of Cu(II) and Cr(VI), as examples of a cation and an oxyanion found in high concentrations in water following wildfire events near VALL. High decreases in Cu(II) concentration (up to 92%) was observed in solution while Cr(VI) showed limited decrease (up to 13%) in concentration after 180 mins of reaction. X-ray photoelectron spectroscopy (XPS) analyses detected increased association of Cu(II) on the near surface region of the reacted ash from the sorption experiments compared to the unreacted ash. The results from this investigation suggest that dissolution and sorption processes should be considered to understand the transport of metals in water following wildfires. This study provides relevant insights about the potential effects of metals transported by wood ash on water quality that have important implications for post-fire recovery and response strategies

Keywords: Wildfires, Wood Ash, Metal Reactivity, Dissolved Organic Carbon, Metal Mobility, Metal Sorption, Post-fire Recovery, Valles Caldera National Preserve

## TABLE OF CONTENTS

TABLE OF CONTENTS.....	v
BACKGROUND, JUSTIFICATION, AND OBJECTIVES .....	1
MATERIALS AND METHODS.....	3
Field Sampling and Ash Preparation .....	3
Acid Digestion and Solution Chemistry Analyses.....	3
Batch Experiments for DOC concentration and metal dissolution .....	4
Batch sorption experiments of Cu(II) and Cr(VI) onto 350°C Pine Ash .....	5
Solid Phase Analyses. (SEM/EDX, EPMA, XRD, XPS) .....	5
Statistical Analysis.....	6
RESULTS AND DISCUSSION .....	6
Water Quality and Sediment Data from Valles Caldera .....	6
Acid Extractable Metal Content in Wood Exposed to 60°C, 350°C, and 550°C. ....	8
Metal and DOC Leachates from Pine Ash (350°C and 550°C) Reacted with Water .....	9
Sorption to 350°C Pine Ash. ....	10
Solid Phase Analyses of Unreacted and Reacted 350°C Pine Ash.....	11
CONCLUSIONS AND RECOMMENDATIONS .....	13
REFERENCES .....	15
APPENDICES .....	21

## LIST OF FIGURES AND TABLES

Figure 1. Materials and methods used for the analysis .....	4
Figure 2. Acid-extractable concentrations of metals across different tree species of (A) pine, (B) spruce and (C) aspen. ....	8
Figure 3. Dissolved organic carbon (DOC) concentration was measured in the leachates from the batch experiments conducted with 350°C and 550°C ash samples of pine, spruce, and aspen.....	9
Figure 4. Results from the metal sorption experiments .....	11
Figure 5. <i>High resolution Cu 2p XPS spectra</i> .....	12
Table 1. Elemental content of water and soil samples from the East Fork.....	7





## JUSTIFICATION OF WORK PERFORMED

Post-fire storm events in watersheds can cause the transport of wood ash into nearby streams, which has detrimental impacts on water quality. In the United States, the forests in the southwestern regions have seen increased occurrences of large intensity wildfires because of worldwide effects of climate change.<sup>1-3</sup> The Valles Caldera National Preserve (VALL) in north central New Mexico is an example of a site with frequent wildfire activity in recent years.<sup>4</sup> Two major wildfires have affected the East Fork Jemez River watershed in VALL since 2011: (1) The Thompson Ridge wildfire burned 23,965 acres in VALL in 2013<sup>5</sup> and (2) The catastrophic Las Conchas fire, one of the largest in New Mexico history, which burned over 156,000 acres in the Jemez Mountains in 2011.<sup>6</sup> Post-fire runoff of debris and ash in the Rio Grande, following thunderstorms over the burned area, caused turbidity peaks of over 1000 nephelometric turbidity units (NTU) and sags in dissolved oxygen (DO) and pH.<sup>7</sup> The total concentration of Al and Cu in the Rio Grande following the Las Conchas fire were above aquatic life criteria for both metals.<sup>8</sup> Additionally, post fire runoff caused the transport of organic matter and nutrients ( $6 \times$  background levels for  $\text{NO}_3\text{-N}$  and  $100 \times$  background levels for  $\text{PO}_4$ ) with debris and ash in the VALL, which significantly affected the quality of water supplied to nearby communities.<sup>7,9</sup> Information on the composition and reactivity of metals associated with wood ash is important to better understand the potential impacts on water quality and assess the viability of current treatment methods.

While previous studies have characterized metals and organic matter in wood ash and soil,<sup>10-13, 70-71</sup> the specific mechanisms controlling postfire metal mobilization remain poorly understood. Elevated concentrations of metals have been observed in sediments and surface water in fire-affected watersheds, for several months after the fire events.<sup>1,14-17</sup> Recent studies have linked water extractable organic matter (WEOM) from burned soil<sup>10,18</sup> and ash<sup>19</sup> to the formation of disinfection byproducts (DBPs).<sup>20,21</sup> Temperature is a particularly important factor that affects the elemental composition and mineralogy of wood ash.<sup>22-24</sup> For example, a previous study from our group identified the presence of Ca, Mg, Al, Fe and Mn as metal-bearing carbonate and oxide phases in wood ash burned at  $550^\circ\text{C}$ .<sup>12</sup> Results from laboratory batch experiments suggest that these metal-bearing phases are readily water soluble, but the re-adsorption of these metals to ash can occur in later times of the experiments.<sup>12</sup> Although this study provides valuable insights to the presence of metal-bearing phases in the ash and their potential effects on metal re-adsorption, knowledge of the specific processes affecting metal dissolution and sorption in wood ash is still limited.

More mechanistic investigations have been reported in the literature related to the reactivity of biochar, a material similar to wood ash in composition.<sup>25,26</sup> Biochar is a natural sorbent and increasingly is

applied in environmental remediation of organic and inorganic contaminants.<sup>27-29</sup> The sorption of Cu(II) to organic functional groups of biochar in water can occur at pH below 7.<sup>30</sup> However, Cu-associated phases like azurite ( $\text{Cu}_3(\text{CO}_3)_2(\text{OH})_2$ ) and tenorite ( $\text{CuO}$ ) precipitate within the biochar surface at pH higher than 7.<sup>30</sup> Sorption between positively charged ions and negatively charged biochar is an effective mechanism for immobilizing metals in soil.<sup>29,31,32</sup> The immobilization of Cr(VI) through biochar sorption is reduced significantly at pH 5 and above due to the negative charge of chromate oxyanions and the biochar surface.<sup>33, 34,35</sup> Enhanced sorption of other oxyanions like As<sup>36,37</sup> and Sb<sup>38</sup> has been observed in biochar-treated soil. Similar mechanistic studies are necessary to identify sorption, precipitation, and dissolution reactions facilitated by wood ash that can affect post-fire metal mobility.

The main objective of this study is to investigate the interfacial processes affecting wood ash reactions with water by integrating laboratory experiments, spectroscopy, microscopy, and aqueous chemistry methods. Soil and surface water chemistry from burned areas of VALL provide environmental context for the study. The release of metals and dissolved organic carbon (DOC) was assessed in batch experiments reacting laboratory-burned wood ash with water. Additional experiments were conducted to investigate sorption processes that affect ash-metal interactions. The focus of this study is to identify interfacial physical-chemical processes that have not been extensively studied in the existing wildfire literature. The results from this investigation have relevant implications for the improvement of post-fire responses in affected watersheds.

## REVIEW OF METHODS USED

### Field Sampling and Ash Preparation

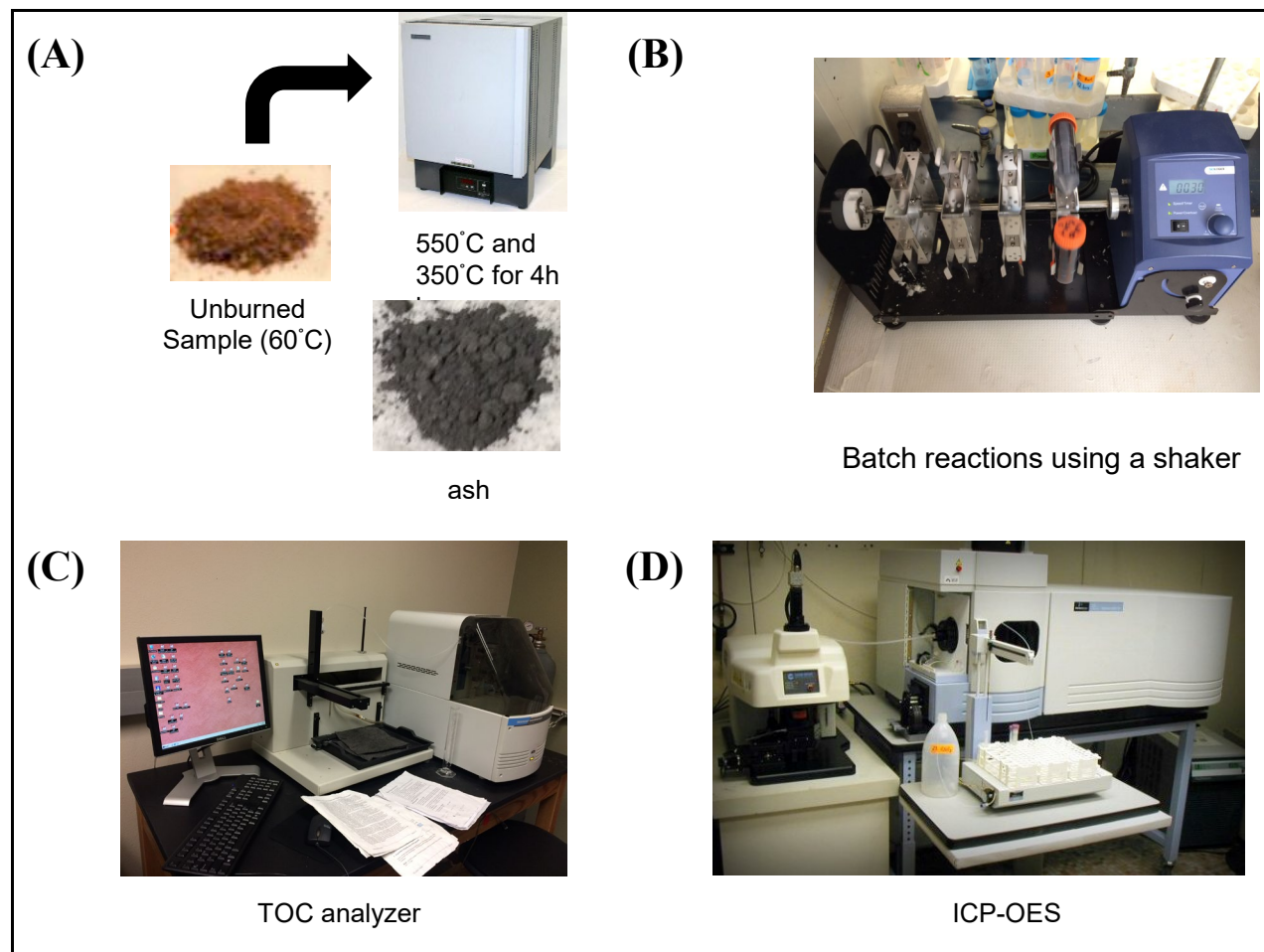
The East Fork Jemez River and adjacent areas were affected by the Las Conchas and Thompson Ridge wildfires in 2011 and 2013. There is a lack of information about distribution of metals in soils, water, and wood from the VALL. Water and soil sampling were done to assess the current availability of metals in this fire-affected watershed. Wood was collected from a nearby unburned area to experiment with laboratory burn temperatures. Additional details about sampling methods are provided in the Appendices section. Surface water samples were collected as grab samples in 125 mL polypropylene bottles after three rinses. Samples for dissolved metals analysis were filtered through a 0.45  $\mu\text{m}$  filter. Samples for metals' analysis were acidified to a pH of 2 with nitric acid. Soil samples were collected using a soil auger down to 6 inches and homogenized prior to preparation for analysis.

The vegetation in the VALL is dominated by different species of pine, spruce, aspen, and oak.<sup>39</sup> Wood samples of Ponderosa Pine, Colorado Blue Spruce, and Quaking Aspen were collected from higher elevation mixed coniferous forest areas that have a fire disturbance history from Las Conchas and other fires.<sup>12,40</sup> This area in VALL is also densely forested, undergoes prescribed burns periodically, and accounts for approximately 25% of the precipitation volume in the Caldera.<sup>41</sup> From this point on, we will call these tree species simply pine, spruce, and aspen. The collected wood samples were crushed and then oven dried at 60°C for 48h before burning. The dried samples were burned in a laboratory muffle furnace at 350°C (moderate burn) and at 550°C (high burn) for 4 hours to prepare ash.

### Acid Digestion and Solution Chemistry Analyses

Wood samples were acid digested in triplicates ( $n = 3$ ) at 95°C for 4 hours using Aqua Regia [2 mL  $\text{HNO}_3$  (67-70%) + 6 mL  $\text{HCl}$  (34-37%), trace metal grade]. Following heating, acid extracts were diluted with 18M $\Omega$  water to reach a volume of 50 mL. Processing of all aqueous samples (water, soil and wood) for this study was done by filtering through a 0.45  $\mu\text{m}$  filter, acidifying with 2%  $\text{HNO}_3$ , and refrigerating at 4°C until further solution chemistry analyses. Inductively Coupled Plasma-Optical Emission Spectrometry (ICP-OES, PerkinElmer Optima 5300DV) was used for detection of concentrations of major elements (Ca, Mg and K). Minor or trace elements were analyzed using Inductively Coupled Plasma-Mass Spectrometry (ICP-MS, PerkinElmer NexION 300D). Both the ICP-OES and ICP-MS analyzed an internal indium standard and were calibrated using a 5-point calibration curve. The quality of the results was ensured with proper quality control and quality assurance standards. The detection limits for the ICP-OES and ICP-MS for specific elements are shown in Table S7. Dissolved organic carbon in

these samples was measured using a Shimadzu TOC-5050A TOC analyzer. The information in the methods section has been illustrated in Figure 1.



**Figure 1.** Materials and methods used for the analysis

### **Batch Experiments for DOC concentration and metal dissolution**

For DOC dissolution experiments, batch reactors were operated in triplicates by reacting 0.1g sample of 350°C and 550°C pine, spruce and aspen ash with 30 mL of 18M $\Omega$  deionized water. Replicates (n=3) were sampled at 0, 4, 24 and 72 hours and were analyzed using a Shimadzu TOC-5050A TOC analyzer, following 5310-C persulfate-ultraviolet (UV) method.<sup>42</sup> For metal dissolution experiments, 0.1g samples of 350°C and 550°C pine ash were reacted with 30 mL of 18 m $\Omega$  water. Samples were collected at 0, 4, 24 and 72 hours, centrifuged at 3000 rpm for 15 minutes and processed for further ICP analyses.

## **Batch sorption experiments of Cu(II) and Cr(VI) onto 350°C Pine Ash**

Batch sorption experiments in triplicates were conducted to investigate the effect of 350° pine ash on mobilization of Cu(II) and Cr(VI) in water. We selected Cu(II) and Cr(VI) as examples of a cation and an oxyanion that could negatively impact surface waters. Additionally, elevated concentrations of these metals were found in surface water following wildfire events near VALL.<sup>8,43</sup> It is also worth noting that Ponderosa Pine dominates the mixed coniferous forests, which reportedly constitute over 40% of the area in Valles Caldera.<sup>39</sup> Thus, we considered 350°C Pine ash for these additional sorption experiments due to its relevant implications for the study area. The Brunauer-Emmett-Teller (BET) specific surface area for the 350°C and 550°C pine ash samples were measured using a Gemini 2360 V5 surface area analyzer. The zeta potential, which measures the surface charge of a solid, of the 350°C pine ash was determined using a Malvern Zetasizer. Stock solutions (1000 ppm) of Cr(IV) and Cu(II) were prepared by dissolving analytical grade (>99% purity) K<sub>2</sub>Cr<sub>2</sub>O<sub>7</sub> and CuCl<sub>2</sub>·2H<sub>2</sub>O in 18MΩ water. For the experiment, 0.1g sample of 350°C pine ash was reacted separately with 10 μM of Cu(II) and Cr(VI) stock solutions mixed in 50mL of 18MΩ water. The concentrations of Cu(II) and Cr(VI) were chosen to reflect levels measured in water samples collected during storm events after the Cerro Grande fire.<sup>43</sup> The pH was adjusted to 7.0±0.2 using 2% HCl. Control experiments were done at pH 7.0±0.2 for Cu(II) and Cr(VI). The 50mL tubes were shaken at 30 rpm to facilitate the reaction. Samples were collected at 0, 4, 24 and 72 hours, centrifuged at 6000 rpm for 3 min, and were processed for further solution chemistry analyses using ICP-MS.

## **Solid Phase Analyses (SEM/EDX, EPMA, XRD, XPS)**

Solid phase analyses were performed on the unreacted and reacted 350°C pine ash from the batch sorption experiments by applying X-ray photoelectron spectroscopy (XPS), scanning electron microscopy coupled to energy dispersive X-ray spectroscopy (SEM/EDX), electron probe microanalysis (EPMA), and X-ray diffraction (XRD). Elemental composition and the oxidation states in the near surface (5-10 nm) were acquired using a Kratos Axis DLD Ultra X-ray photoelectron spectrometer. A monochromatic Al K $\alpha$  source was used, operating at 225W with no charge compensation. The Cu 2p spectra from reference Cu samples were used to identify the species of Cu present on the near surface region of the reacted ash sample. Reference Cu samples [Cu metal, Cu(I, II) oxide and Copper(II) carbonate basic] were purchased from Sigma Aldrich, Strem Chemicals and Alfa Aesar respectively. All the chemicals were >99% pure except the Copper(II) carbonate basic ( $\geq$ 95% purity). The high-resolution spectra, along with the binding energies obtained for the Cu 2p regions for these reference materials, are shown in Appendix S9. Curve fitting and quantification were performed using CasaXPS software. Spectra of all the samples were calibrated using gold powder deposited on each sample with respect to the Au 4f peak position at 84 eV.

Electron scattering background was removed using a Shirley background; curve fitting of spectra was done using a 70% Gaussian/30% Lorentzian [GL (30)] line shape. Qualitative mapping of the ash samples was done using an electron probe microanalyzer (EPMA) using wavelength dispersive X-ray spectroscopy (WDS). A JEOL JXA-8200 Super-Probe was used, operating at 10 kV with a 10  $\mu\text{m}$  probe diameter and 30 nA probe current.

### **Statistical Analysis**

Univariate data analysis was performed using the statistical software R.<sup>44</sup> The statistical package in OriginPro<sup>45</sup> was used for Principal Component Analysis (PCA). Due to the non-normality of the data, nonparametric tests for differences in acid extractable metal concentrations ( $\log_{10}$  transformed to reduce skewness in distribution) were performed to differentiate among 3 tree species (pine, spruce, aspen) and among 3 temperatures (60°C, 350°C and 550°C). A Kruskal-Wallis test was performed to determine if the tree species and the temperatures differ significantly (defined as  $p < 0.05$ ) with respect to metal concentrations ( $\log_{10}$  transformed). The Wilcoxon rank sum test was used to do pairwise comparisons of all the samples to test for significant differences between tree species and temperatures (defined as  $p < 0.05$ ). PCA was performed to better understand the total chemical correlations among ash samples of all tree species in triplicates and acid extractable metal concentrations.

## **DISCUSSION OF RESULTS AND THEIR SIGNIFICANCE**

### **Water Quality and Sediment Data from Valles Caldera**

The presence of Cu, Cr, Fe, Zn, and Mn was observed in water from the wildfire affected East Fork Jemez River and in soils exposed to varying burn severities upslope from the East Fork Jemez River headwaters (Table 1, Appendix A). Maximum total (non-filtered) concentrations of Cu (37.4  $\mu\text{g L}^{-1}$ ) and Fe (2650  $\mu\text{g L}^{-1}$ ) in the water samples collected from site 2 and Zn (352  $\mu\text{g L}^{-1}$ ), from site 3 were above the United States Environmental Protection Agency (USEPA) standards for acute or chronic exposure values for aquatic life in freshwater (Table 1, Appendix F). Total Cr (105  $\mu\text{g L}^{-1}$ ) in the water samples collected from site 2 exceeded the USEPA standards for acute or chronic exposure for both Cr(III) (74  $\mu\text{g L}^{-1}$ ) and Cr(VI) (11  $\mu\text{g L}^{-1}$ ). In a 2001 study by the New Mexico Environment Department, Al, pH, dissolved oxygen (DO), and turbidity in the East Fork Jemez river were listed as exceeding the Total Maximum Daily Load, while metals, such as Cu, Cr and Zn were found to be less than instrument detection limit,<sup>46,47</sup> lower than found in this study. Average concentrations of major and trace elements ( $\text{mg kg}^{-1}$ ) in non-anthropogenically affected soils in the US estimated by Burt et al.<sup>48</sup> (shown in Appendix

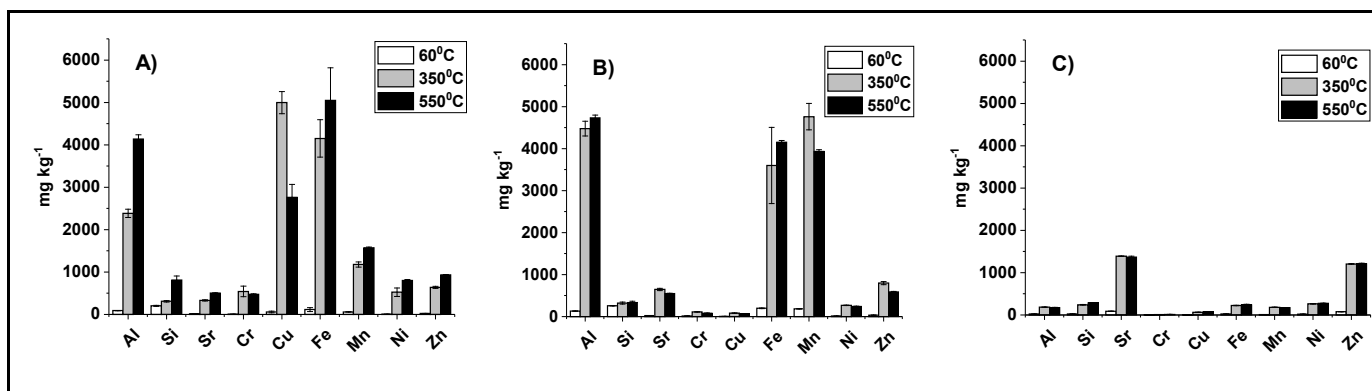
F) were used to evaluate the metal concentrations in the soil samples collected along the river reaches. Fe was the most abundant metal with concentrations ranging from 4980 mg kg<sup>-1</sup> to 9850 mg kg<sup>-1</sup>. Cu concentration in the collected soil samples from site V1, V2, and V3 ranges from 44.2 mg kg<sup>-1</sup> to 261 mg kg<sup>-1</sup>, higher than the average Cu concentration (24.7 mg kg<sup>-1</sup>) of non-anthropogenic affected soils in the US (Appendix F). Concentrations of trace metals in water and soil near a burned watershed can increase from the addition of ash and debris by storm water runoff. For example, after the Cerro Grande fire in 2000, elevated concentrations of total Cu (610 µg L<sup>-1</sup>) and total Cr (510 µg L<sup>-1</sup>) were measured in post fire runoff water samples collected from the burned watersheds near Guaje Canyon, which is close to the Los Alamos National Laboratory.<sup>43</sup> Additional laboratory experiments were done to determine the concentrations of metals in oven dried wood and ash and to assess the reactivity of wood ash upon reaction with 18MΩ water.

Site	pH	Alkalinity (mg L <sup>-1</sup> )	TOC (mg C L <sup>-1</sup> )	Water elemental content (µg L <sup>-1</sup> )				
				Cu Total	Cr Total	Fe Total	Zn Total	Mn Total
Site 1	7.17 - 8.44	30.5 - 42.0	0.80 - 2.00	2.81 - 16.7	BDL <sup>b</sup> - 105	289 - 932	52.2 - 103	6.90 - 57.2
Site 2	7.11 - 8.06	31.0 - 38.3	1.60 - 10.8	5.44 - 37.4	BDL - 8.20	465 - 2650	41.4 - 335	8.83 - 146
Site 3	6.55 - 7.66	24.1 - 43.8	4.00 - 10.3	7.93 - 23.4	BDL - 48.4	38.2 - 677	57.4 - 352	1.58 - 39.2
Site 4	6.48 - 8.01	38.7 - 43.7	4.60 - 11.3	5.31 - 21.7	BDL - 16.5	358 - 757	60.7 - 241	6.56 - 22.4
Site 5	6.48 - 7.97	33.8 - 40.9	3.20 - 11.0	BDL - 25.2	BDL - 11.5	331 - 948	72.8 - 135	BDL - 44.4
Soil sampling sites				Soil elemental content (mg kg <sup>-1</sup> )				
				59.4 - 86.9	10.9 - 35.3	7800 - 9620	13.0 - 38.5	219 - 319
				71.3 - 89.9	9.25 - 20.4	4980 - 9850	10.2 - 31.4	50.8 - 194
				44.2 - 261	11.0 - 17.2	5050 - 7940	14.9 - 37.9	92.7 - 139
				7.16 - 17.5	5.81 - 13.3	109 - 221	19.5 - 35.2	260 - 347
				5.97 - 18.6	4.96 - 15.2	86.4 - 190	22.2 - 54.2	179 - 344
				7.97 - 13.9	5.31 - 11.3	102 - 184	30.8 - 39.4	217 - 454
<sup>a</sup> Aqueous and soil elemental content measured with ICP-OES and ICP-MS <sup>b</sup> BDL = Below detection limit								

**Table 1.** Elemental content of water (site 1 to 5) and soil (site V1 to V3) samples<sup>a</sup> from the East Fork Jemez River within the Valle Grande area in VALL. Sites V4 to V6 contain soil samples from the hill slope of the Sierra de Los Valles dome located near the headwaters of the river. Ranges of concentrations (minimum to maximum) for each site are shown

## Acid Extractable Metal Content in Wood Exposed to 60°C, 350°C, and 550°C

We compared the acid extractable metal contents using Aqua Regia in 9 samples (pine, spruce, and aspen at 60°C, 350°C and 550°C, Figure 2). Acid extractable median metal concentrations at 350°C (moderate burn) and 550°C (high burn) for all tree species (e.g., pine, spruce, and aspen) were significantly higher ( $p < 0.05$ , Appendix B, C) compared to oven dried wood at 60°C (unburned). The acid-extractable metal concentrations for all samples at 60°C, 350°C, and 550°C are shown in Appendix A. Pairwise comparisons suggest that metal contents in oven dried wood at 60°C for pine, spruce and aspen were not significantly different from each other ( $p > 0.05$ , Appendix B, C). Among the ash samples at 350°C and 550°C, pine and aspen were significantly different ( $p < 0.05$ , Appendix C) from each other with respect to acid extractable metal concentrations. Principal Component Analysis (PCA, Appendix C) suggests that 350°C and 550°C Pine ash samples were associated with high concentrations of most of the metals (Cu, Cr, Si, Ni, Fe, K and Mg). High concentrations of Ca, Sr and Zn were associated with 350°C and 550°C aspen ash samples, while 350°C and 550°C spruce ash samples were associated with high concentrations of Mn, Al, and Fe.



**Figure 2.** Acid-extractable concentrations (mean  $\pm$  SD) of 9 metals varied across different tree species of (A) pine, (B) spruce and (C) aspen. The major elements (Ca, Mg and K) were predominant in all tree species at 60°C, 350°C, and 550°C (Appendix A). Ash produced at both 350°C (moderate burn) and 550°C (high burn) contained higher metal concentrations than in samples dried at 60°C (unburned) for all species.

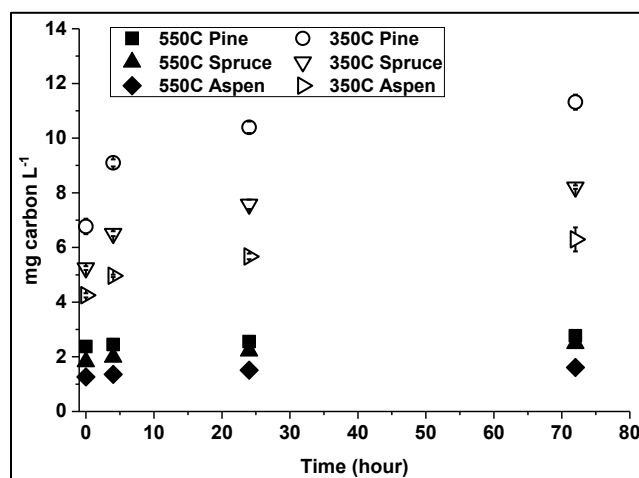
Major elements (Ca, Mg, K) were found to be predominant in oven dried wood (60°C) and in ash samples (350°C and 550°C) for all tree species (Appendix A), consistent with findings for wood<sup>49</sup> and wood ash<sup>12,50</sup> from previous studies. Pine ash showed higher concentrations with increasing temperatures for major elements (Ca, Mg and K) and for heavy metals such Al, Fe, Mn, and Ni (Appendix A), consistent with findings from a previous study conducted on Lodgepole Pine.<sup>51</sup> The concentration of Cu in pine ash ( $4997 \pm 262$  mg kg<sup>-1</sup> at 350°C and  $2765 \pm 302$  mg kg<sup>-1</sup> at 550°C) was higher than previously reported values for Pine ash.<sup>12,51</sup> Due to the dominance of pine tree species in the forests of western United States, much of



the existing literature has focused on the metal and dissolved organic carbon (DOC) composition of ash produced from different species of Pine (e.g., Ponderosa and Lodgepole).<sup>12,18,52-54</sup> Given that the highest concentrations for most metals were associated with pine, we conducted additional experiments with pine ash to assess the release of dissolved organic carbon and other metals over time.

### Metal and DOC Leachates from Pine Ash (350°C and 550°C) Reacted with Water

Metal leaching experiments were conducted to observe the dissolution and desorption of selected metals (Cr, Ni, Fe, Cu, and Zn) in reaction with 350°C and 550°C pine ash in deionized water. We decided to use de-ionized water as a proxy for pristine natural waters such as rainwater to understand potential reactions after storm events. The data for metal concentrations in solution over time are presented in Appendix K. Dissolution of metal-bearing phases caused a rapid increase in the pH of water, measured at  $10.0 \pm 0.5$  for the duration of the experiment. Less than 3% by mass [determined in acid extractable analysis (Appendix A)] of Cr, Ni, Fe, Cu, and Zn were released in solution after 72 hours of reaction. Metals like Cu, Fe, Zn, and Ni showed initial increase followed by decrease in metal concentration over time for both the 350°C and 550°C pine ash. Limited fluctuations in the concentration of Cr released in solution were observed over time (Appendix K). The high pH and alkalinity in these experiments (Appendix K) are likely due to the dissolution of metal-bearing carbonate and oxide phases, such as calcite, quartz, and whewellite [ $\text{Ca}(\text{C}_2\text{O}_4) \cdot \text{H}_2\text{O}$ ], which were identified by XRD analysis in the unreacted 350°C Pine ash (Appendix L). A previous study from our group also identified the presence of calcite and other metal-bearing phases in ash burned at 550°C.<sup>12</sup>



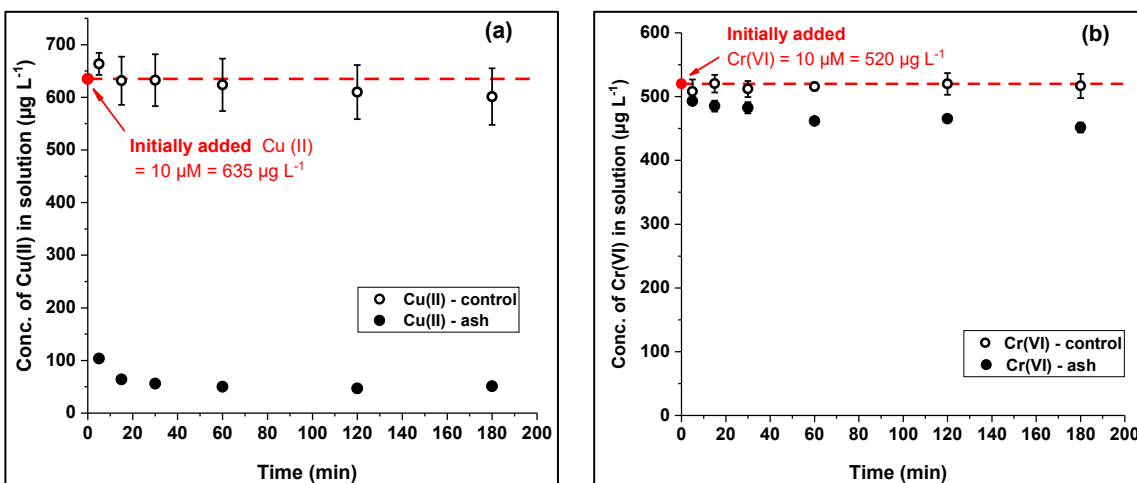
**Figure 3.** Dissolved organic carbon (DOC) concentration was measured in the leachates from the batch experiments conducted with 350°C and 550°C ash samples of pine, spruce, and aspen. DOC concentration ( $\text{mg carbon L}^{-1}$ ) at 0, 4, 24 and 72 hours ( $n=3$ ) is shown here.

Higher DOC concentrations (4.25 to 11.3 mg carbon L<sup>-1</sup>) were detected after reacting 350°C ash with 18 MΩ water, compared to DOC concentrations obtained for 550°C ash (1.27 to 2.77 mg carbon L<sup>-1</sup>) (Figure 3). Among the ash samples, 350°C pine ash released the highest concentration of DOC after 72 hours (11.3±0.28 mg carbon L<sup>-1</sup>). The decrease in DOC concentration from 350°C to 550°C ash suggests that a greater loss of organic matter occurs at a higher burning temperature, consistent with findings from previous studies.<sup>10,12</sup> The range of DOC concentrations (1.27 to 11.3 mg carbon L<sup>-1</sup>) measured for 350°C and 550°C ash samples in this study are consistent with those reported in previous studies from field<sup>15,18</sup> and laboratory studies.<sup>10</sup> The alteration of DOM with increasing temperature from pine ash has been studied previously. Wang et al.<sup>54</sup> observed decreased reactivity of the ash in forming DBPs such as trihalomethane (THM) and chloral hydrate (CHD) with increasing temperature from 50°C to 400°C. The DOC loss at higher temperatures for ash in this study is comparable to that observed in laboratory heated soil by Cawley et al.<sup>10</sup> Thus, the temperature dependent variability for both ash and soil can have implications in terms of variable loading of DOM and DBP precursors from different burn conditions associated with wildfires and prescribed fires, as suggested by others.<sup>10,54</sup> Based on the statistical analyses for the results from acid-extractable elemental analyses and the DOC concentration of leachates, 350°C pine ash was selected for additional sorption experiments.

### **Sorption to 350°C Pine Ash**

We further explored the sorption of Cu(II) (a cationic metal) and Cr(VI) (an oxyanion) to wood ash in batch sorption experiments. The 350°C pine ash was selected for the sorption experiments because it had the highest concentration of Cu (4997 ± 262 mg kg<sup>-1</sup>), Cr (543 ± 124 mg kg<sup>-1</sup>), and DOC (11.3 ± 0.28 mg carbon L<sup>-1</sup>) [Figure 1 and Figure 2]. Zeta potential measurements for the 350°C Pine ash showed increasingly negative surface charge with increasing solution pH (Appendix A), similar to another carbon-based material like biochar.<sup>55,56</sup> The surface area of Pine ash increased from 36.9 m<sup>2</sup>/g at 350°C to 294.4 m<sup>2</sup>/g at 550°C (Appendix D). Previously, Mendonça and others<sup>55</sup> reported an increase in surface area due to creation of micropores for biochar burned at 400°C and 600°C.

We observed more than 80% decrease initially in Cu(II) concentration in solution (Figure 3a), as indicated by measured Cu(II) concentration (103.6 ± 3.1 µg L<sup>-1</sup>) after 5 mins of reaction and up to 92% decrease after 180 mins of reaction. Cu(II) concentration in the control (test tube with no ash) decreased only 5%, to 601.2 ± 53.8 µg L<sup>-1</sup> after 180 mins of reaction from the initially added concentration of 635 µg L<sup>-1</sup>. In experiments with Cr(VI), low decrease in Cr(VI) concentration was observed, as the measured concentration after 180 mins was 451.7 ± 7.8 µg L<sup>-1</sup>, representing only a 13% decrease from the initially added Cr(VI) of 520 µg L<sup>-1</sup> (Figure 3b). Cr(VI) showed negligible decrease in concentration in the Cr(VI)-control experiment (Figure 3b).



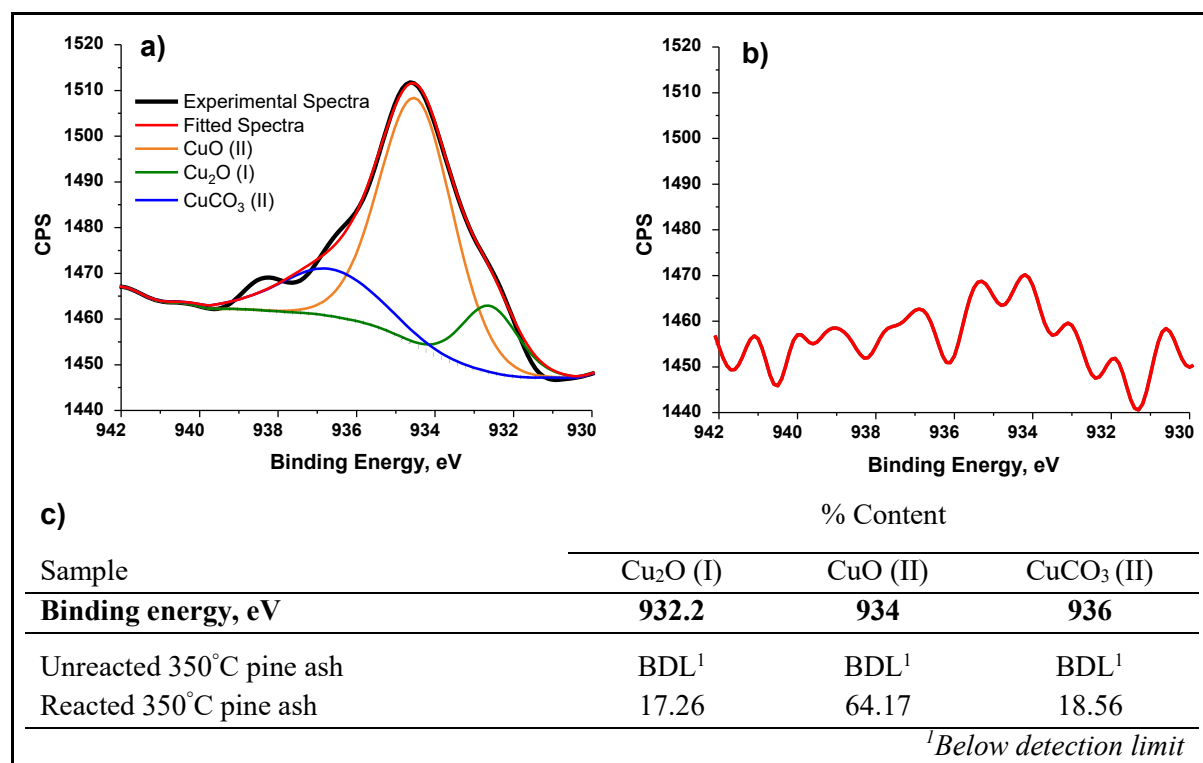
**Figure 4.** Results from the metal sorption experiments ( $n=3$ , sampling interval = 5 min, 15 min, 30 min, 1 hr, 2 hours, and 3hrs) conducted by reacting  $10 \mu\text{M}$  of (a) Cu(II) and (b) Cr(VI) separately in a solution containing 0.1g of  $350^\circ\text{C}$  Pine ash with 50mL of  $18\text{M}\Omega$  water. Results from the control experiments without the ash are included in the figures (a) for Cu(II) and (b) for Cr(VI).

The different response of Cu(II) and Cr(VI) concentration during the sorption experiments suggests that high Cu(II) association to ash occurred due to possible electrostatic attraction of the positively charged Cu(II) to the negatively charged ash surface. The effect of sorption capacity of the carbonate phases in wood ash in reacting with cations such as  $\text{Ca}^{+2}$ ,  $\text{Mg}^{+2}$ ,  $\text{Al}^{+3}$ ,  $\text{Mn}^{+2}$ ,  $\text{Fe}^{+2}$ ,  $\text{Pb}^{+2}$ ,  $\text{Cu}^{+2}$ ,  $\text{Zn}^{+2}$ , and  $\text{Cd}^{+2}$  has been discussed in other studies.<sup>12,13</sup> This is a relevant property of wood ash that should be considered when investigating the persistence of metals such as Cu, Pb, Ni, Fe, and Zn associated with ash and debris in wildfire affected watersheds, as reported in several post-fire investigations.<sup>57-59</sup> The low sorption of Cr(VI) observed in this study is consistent with other studies reporting low sorption rates for As(V), Cr(VI) and Se(VI) to carbon based materials at pH 5.0 and above.<sup>60-62</sup> For example, a recent study by Alam et al. observed over 90% removal of Cd(II) and below 20% removal for Se(VI) at pH 6.0 and above, using biochar as an adsorbent.<sup>60</sup> At the experimental pH of  $7.0 \pm 0.2$  used in this study, Cr(VI) is expected to exist in solution as stable oxyanion forms of chromate ( $\text{CrO}_4^{2-}$ ) and hydrogen chromate or bichromate ( $\text{HCrO}_4^-$ ).<sup>63</sup> Therefore, the electrostatic repulsion between the negatively charged ash surface and Cr(VI) oxyanions can account for the low decrease in Cr(VI) concentration in solution. The association of Cu(II) in the unreacted and reacted  $350^\circ\text{C}$  Pine ash solids were further analyzed using microscopy and spectroscopy.

### Solid Phase Analyses of Unreacted and Reacted $350^\circ\text{C}$ Pine Ash

SEM analysis detected the presence of Cu on  $350^\circ\text{C}$  pine ash before and after exposure to batch experiments (Appendix M). For example, EDS spectra of a Cu grain showed 69.51 weight % of Cu for

the unreacted ash, and 63.55 weight % of Cu for the reacted ash. SEM/EDS results confirmed the high Cu concentration ( $4997 \pm 262 \text{ mg kg}^{-1}$ ) measured from the acid extraction analyses. Electron microprobe mapping detected low level of Cu (0.012%) associated with the  $\text{Ca}^{+2}$  minerals in the reacted ash (Appendix N), and concentrations below the detection limit for the unreacted ash. The predominant form of the  $\text{Ca}^{+2}$  mineral is most likely calcite ( $\text{CaCO}_3$ ), given the presence of 76-78 wt% of calcite in the reacted sample from the XRD analysis (Appendix L). Given that Ca is a macronutrient in plants,  $\text{Ca}^{+2}$  minerals in the form of CaO and  $\text{CaCO}_3$  are abundant across a variety of plant cells.<sup>64,65</sup> XRD analyses on reacted and unreacted samples indicated the presence of quartz and calcite as predominant mineral phases (Appendix L). While microscopy analyses identified the presence of Cu, it was challenging to obtain specific information about the association of Cu on the reacted ash surface from these analyses. Thus, additional analyses using XPS were done to measure the signal of Cu 2p on the “near-surface” region to identify the possible association of Cu to ash after reaction in batch sorption experiments.



**Figure 5.** High resolution Cu 2p XPS spectra for the (a) Reacted 350°C Pine ash sample. (b) The spectra for the unreacted 350°C pine ash sample was noisy and therefore, could not be fitted with curve fitting analysis. (c) Percentages of different oxidation states in the Cu 2p spectra for the reacted ash determined by using reference Cu 2p spectra for CuO,  $\text{CuCO}_3$ ,  $\text{Cu}_2\text{O}$  and Cu metal.

Results from a XPS survey scan revealed that 0.11% Cu 2p was present in the reacted ash, suggesting that Cu is associated at the top 5-10 nm of the ash “near surface” region (Appendix E). However, the Cu 2p % for the unreacted ash was below the detection limit (Appendix E). So, the high

resolution Cu 2p peak obtained for the unreacted ash was noisy and could not be used for curve fitting analyses (Figure 5). Curve fitting of high resolution XPS Cu 2p spectra obtained for the reacted sample was conducted using reference spectra for CuO, CuCO<sub>3</sub>, Cu<sub>2</sub>O, and Cu metal as indicated in the Materials and Methods section. Curve fitting analysis suggests that the main species of Cu present on the reacted ash are: Cu(II) in the form of CuO (64.2%) and CuCO<sub>3</sub> (18.6%), and Cu(I) in the form of Cu<sub>2</sub>O (17.3%) (Figure 5).

The association of Cu on the reacted 350°C Pine ash near surface region suggests a likely surface controlled process involved in the removal of Cu(II) in the sorption experiments. Curve fitting analysis of C 1s high resolution spectra showed an increase in the percentages of C\*-CO<sub>x</sub>, C=O and C-OH bonds in the reacted ash (Appendix O). The presence of surface functional groups (-C=O, -COOH) in ash can act as negatively-charged binding sites for positively charged cations. The removal of cationic metals such as Cu<sup>+2</sup> and Cd<sup>+2</sup> through associations with surface functional groups of biochar has been discussed in the literature.<sup>30,66,67</sup> These properties are also relevant to better understand the effect of burned soil and ash on post fire mobilization of heavy metals.

## CONCLUSIONS AND RECOMMENDATIONS

The results from this investigation indicate how metal and DOC content associated with ash burned at different temperatures (350°C and 550°C) can differ for spruce, aspen, and pine. This is a relevant outcome that may have implications when considering the wide variation in vegetation across large watersheds when assessing response to wildfire events. Ash burned at 350°C contained higher DOC concentration in water compared to ash burned at 550°C. This observed increase may have important implications in terms of increased DOC fluxes in post fire watersheds from moderately burned ash and soil reported in previous studies.<sup>15,68</sup> The batch experiments conducted in 18 MΩ water indicate that metals such as Cr, Ni, Fe, Cu, and Zn were dissolved in the initial stages of the experiment, followed by decreases in concentration over the duration of the experiment. This observation is consistent with a previous study suggesting that metal (Ca, Mg, Al, Fe, and Mn) dissolution occurred in initial stages of the batch experiments conducted with ash from pine, aspen and spruce trees from the Caldera, followed by re-association of these metals to ash over time.<sup>12</sup> Sorption experiments conducted in this study indicate that up to 92% of Cu is removed from solution after 180 mins of reaction due to

association of this metal in the 350°C Pine ash surface. A similar behavior is expected for other positive cations such as  $\text{Ca}^{+2}$ ,  $\text{Mg}^{+2}$ ,  $\text{Zn}^{+2}$ ,  $\text{Al}^{+3}$ ,  $\text{Fe}^{+2}$ ,  $\text{Cd}^{+2}$ , and  $\text{Pb}^{+2}$  among others, as suggested in other studies related to wood ash<sup>12,13</sup> and biochar<sup>29,69</sup> reactivity. The results from the metal dissolution and sorption experiments in this study provide insights into the mechanisms of post fire mobilization of cationic metals in burned watersheds. However, oxyanions such as Cr(VI) are expected to have limited association to ash in natural pH conditions and are likely to have higher mobility in watersheds affected by wildfires. Future experiments are necessary to study metal reactivity in wood ash in dynamic flow conditions that allow interactions between ash and sediments in water. This study provides relevant insights on water quality that could be considered for post-fire response and recovery strategies from local authorities.

The current study had some limitations that are important to consider. First, the burning of ash was conducted under controlled laboratory conditions. Thus, it is not possible to directly extrapolate laboratory to natural burning conditions observed in wildfires. Nevertheless, laboratory controlled studies on the release of metals and dissolved organic matter (DOM) from ash<sup>12</sup> and burnt soil<sup>10</sup> have important implications for better understanding the mechanisms related to post fire availability of metals and DOM. Additionally, the batch flow conditions in this study are not representative of the dynamic flow conditions during post fire runoff of ash and sediments. Future experiments are necessary to study metal reactivity in wood ash in dynamic flow conditions to assess interactions between ash and sediments in water. This study provides relevant insights on water quality that could be considered for post fire response and recovery strategies from local authorities.

## SUMMARY

The proposed objective is to investigate the effect of burning intensity on the mineralogy and reactivity of metals associated with wildfire ash. The knowledge generated from this study is vital for long-term recovery of ecosystem and management response after wildfire events. The results from this study will enable the identification of negative effects of wildfires, which are essential to improve post-fire recovery strategies, and to ensure the resilience of our forests and water sources. The work reported in this study has been published in the journal *Environmental Science & Technology*.<sup>72</sup>

## REFERENCES

- (1) Bladon, K. D.; Emelko, M. B.; Silins, U.; Stone, M., Wildfire and the Future of Water Supply. *Environ. Sci. Technol.* **2014**, *48*, (16), 8936-8943.
- (2) Spracklen, D. V.; Mickley, L. J.; Logan, J. A.; Hudman, R. C.; Yevich, R.; Flannigan, M. D.; Westerling, A. L., Impacts of climate change from 2000 to 2050 on wildfire activity and carbonaceous aerosol concentrations in the western United States. *J. Geophys. Res. Atmos.* **2009**, *114*, 2156-2202.
- (3) Westerling, A. L.; Hidalgo, H. G.; Cayan, D. R.; Swetnam, T. W., Warming and Earlier Spring Increase Western U.S. Forest Wildfire Activity. *Science* **2006**, *313*, (5789), 940-943.
- (4) *Fire Regimes of Montane Grasslands of the Valles Caldera National Preserve, New Mexico*; Highlights of JFSP: 06-3-1-27; Joint Fire Science Program (JFSP): Boise, Idaho, 2011; <http://digitalcommons.unl.edu/cgi/viewcontent.cgi?article=1082&context=jfspresearch>
- (5) *Distribution and Transport of Pyrogenic Black Carbon in Soils Affected by Wildfires, Valles Caldera, New Mexico, with Implications for Contaminant Transport*; Report Number: 365; New Mexico Water Resources Research Institute (NMWRI); Las Cruces, New Mexico, 2015; <https://nmwri.nmsu.edu/wp-content/uploads/2015/technical-reports/tr365.pdf>
- (6) Parmenter, R. R.; Oertel, R. W.; Compton, T. S.; Kindschuh, S.; Peyton, M.; Meyer, W.; Caldwell, C.; Jacobi, G. Z.; Myers, O.; Zeigler, M., Fire and floods in the Valles Caldera National Preserve, New Mexico: In *The 2011 Las Conchas Fire impacts on montane species diversity and food webs*, 97th ESA Annual Convention; Portland, Oregon, USA, 2012.
- (7) Dahm, C. N.; Candelaria-Ley, R. I.; Reale, C. S.; Reale, J. K.; Van Horn, D. J., Extreme water quality degradation following a catastrophic forest fire. *Freshwater Biol.* **2015**, *60*, (12), 2584-2599.
- (8) *2011 Las Conchas Fire Impacts to Water Quality in the Rio Grande*; Surface Water Quality Bureau, New Mexico Environment Department; Santa Fe, New Mexico, 2011; <https://www.env.nm.gov/swqb/Wildfire/6.LasConchas-ImpactsToRioGrande2011.pdf>
- (9) Sherson, L. R.; Van Horn, D. J.; Gomez-Velez, J. D.; Crossey, L. J.; Dahm, C. N., Nutrient dynamics in an alpine headwater stream: use of continuous water quality sensors to examine responses to wildfire and precipitation events. *Hydrol. Process.* **2015**, *29*, (14), 3193-3207.
- (10) Cawley, K. M.; Hohner, A. K.; Podgorski, D. C.; Cooper, W. T.; Korak, J. A.; Rosario-Ortiz, F. L., Molecular and spectroscopic characterization of water extractable organic matter from thermally altered soils reveal insight into disinfection byproduct precursors. *Environ. Sci. Technol.* **2016**, *51*(2), 771-779.
- (11) Steenari, B.-M.; Karlsson, L.-G.; Lindqvist, O., Evaluation of the leaching characteristics of wood ash and the influence of ash agglomeration. *Biomass Bioenergy.* **1999**, *16*, (2), 119-136.
- (12) Cerrato, J. M.; Blake, J. M.; Hirani, C.; Clark, A. L.; Ali, A.-M. S.; Artyushkova, K.; Peterson, E.; Bixby, R. J., Wildfires and water chemistry: effect of metals associated with wood ash. *Environ. Sci. Process. Impacts.* **2016**, *18*, (8), 1078-1089.
- (13) Chirenje, T.; Ma, L. Q.; Lu, L., Retention of Cd, Cu, Pb and Zn by wood ash, lime and fume dust. *Water Air Soil Pollut.* **2006**, *171*, (1), 301-314.

- (14) Costa, M. R.; Calvão, A. R.; Aranha, J., Linking wildfire effects on soil and water chemistry of the Marão River watershed, Portugal, and biomass changes detected from Landsat imagery. *Appl. Geochem.* **2014**, *44*, 93-102.
- (15) Emelko, M. B.; Silins, U.; Bladon, K. D.; Stone, M., Implications of land disturbance on drinking water treatability in a changing climate: demonstrating the need for “source water supply and protection” strategies. *Water Res.* **2011**, *45*, (2), 461-472.
- (16) Smith, H. G.; Sheridan, G. J.; Lane, P. N.; Nyman, P.; Haydon, S., Wildfire effects on water quality in forest catchments: a review with implications for water supply. *J. Hydrol.* **2011**, *396*, (1), 170-192.
- (17) Biswas, A.; Blum, J. D.; Klaue, B.; Keeler, G. J., Release of mercury from Rocky Mountain forest fires. *Global Biogeochem. Cycles* **2007**, *21*, (1), GB1002.
- (18) Hohner, A. K.; Cawley, K.; Oropeza, J.; Summers, R. S.; Rosario-Ortiz, F. L., Drinking water treatment response following a Colorado wildfire. *Water Res.* **2016**, *105*, 187-198.
- (19) Wang, J.-J.; Dahlgren, R. A.; Erşan, M. S.; Karanfil, T.; Chow, A. T., Wildfire altering terrestrial precursors of disinfection byproducts in forest detritus. *Environ. Sci. Technol.* **2015**, *49*, (10), 5921-5929.
- (20) Bond, T.; Huang, J.; Templeton, M. R.; Graham, N., Occurrence and control of nitrogenous disinfection by-products in drinking water—a review. *Water Res.* **2011**, *45*, (15), 4341-4354.
- (21) Baghoth, S.; Sharma, S.; Amy, G., Tracking natural organic matter (NOM) in a drinking water treatment plant using fluorescence excitation–emission matrices and PARAFAC. *Water Res.* **2011**, *45*, (2), 797-809.
- (22) Bodí, M. B.; Martín, D. A.; Balfour, V. N.; Santín, C.; Doerr, S. H.; Pereira, P.; Cerdà, A.; Mataix-Solera, J., Wildland fire ash: production, composition and eco-hydro-geomorphic effects. *Earth-Sci. Rev.* **2014**, *130*, 103-127.
- (23) Ulery, A.; Graham, R.; Amrhein, C., Wood-ash composition and soil pH following intense burning. *Soil Sci.* **1993**, *156*, (5), 358-364.
- (24) Misra, M. K.; Ragland, K. W.; Baker, A. J., Wood ash composition as a function of furnace temperature. *Biomass Bioenergy* **1993**, *4*, (2), 103-116.
- (25) Jones, D. L.; Quilliam, R., Metal contaminated biochar and wood ash negatively affect plant growth and soil quality after land application. *J. Hazard. Mater.* **2014**, *276*, 362-370.
- (26) Lucchini, P.; Quilliam, R.; DeLuca, T. H.; Vamerali, T.; Jones, D. L., Increased bioavailability of metals in two contrasting agricultural soils treated with waste wood-derived biochar and ash. *Environ. Sci. Pollut. Res.* **2014**, *21*, (5), 3230-3240.
- (27) Saeed, A.; Akhter, M. W.; Iqbal, M., Removal and recovery of heavy metals from aqueous solution using papaya wood as a new biosorbent. *Sep. Purif. Technol.* **2005**, *45*, (1), 25-31.
- (28) Yang, X.-B.; Ying, G.-G.; Peng, P.-A.; Wang, L.; Zhao, J.-L.; Zhang, L.-J.; Yuan, P.; He, H.-P., Influence of biochars on plant uptake and dissipation of two pesticides in an agricultural soil. *J. Agric. Food Chem.* **2010**, *58*, (13), 7915-7921.



- (29) Ahmad, M.; Rajapaksha, A. U.; Lim, J. E.; Zhang, M.; Bolan, N.; Mohan, D.; Vithanage, M.; Lee, S. S.; Ok, Y. S., Biochar as a sorbent for contaminant management in soil and water: a review. *Chemosphere*. **2014**, *99*, 19-33.
- (30) Ippolito, J.; Strawn, D.; Scheckel, K.; Novak, J.; Ahmedna, M.; Niandou, M., Macroscopic and molecular investigations of copper sorption by a steam-activated biochar. *J. Environ. Qual.* **2012**, *41*, (4), 1150-1156.
- (31) Uchimiya, M.; Wartelle, L. H.; Klasson, K. T.; Fortier, C. A.; Lima, I. M., Influence of pyrolysis temperature on biochar property and function as a heavy metal sorbent in soil. *J. Agric. Food Chem.* **2011**, *59*, (6), 2501-2510.
- (32) Beesley, L.; Marmiroli, M., The immobilisation and retention of soluble arsenic, cadmium and zinc by biochar. *Environ. Pollut.* **2011**, *159*, (2), 474-480.
- (33) Hsu, N.-H.; Wang, S.-L.; Lin, Y.-C.; Sheng, G. D.; Lee, J.-F., Reduction of Cr (VI) by crop-residue-derived black carbon. *Environ. Sci. Technol.* **2009**, *43*, (23), 8801-8806.
- (34) Hsu, N.-H.; Wang, S.-L.; Liao, Y.-H.; Huang, S.-T.; Tzou, Y.-M.; Huang, Y.-M., Removal of hexavalent chromium from acidic aqueous solutions using rice straw-derived carbon. *J. Hazard. Mater.* **2009**, *171*, (1), 1066-1070.
- (35) Dong, X.; Ma, L. Q.; Li, Y., Characteristics and mechanisms of hexavalent chromium removal by biochar from sugar beet tailing. *J. Hazard. Mater.* **2011**, *190*, (1), 909-915.
- (36) Park, J. H.; Lamb, D.; Paneerselvam, P.; Choppala, G.; Bolan, N.; Chung, J.-W., Role of organic amendments on enhanced bioremediation of heavy metal (loid) contaminated soils. *J. Hazard. Mater.* **2011**, *185*, (2), 549-574.
- (37) Zhang, X.; Wang, H.; He, L.; Lu, K.; Sarmah, A.; Li, J.; Bolan, N. S.; Pei, J.; Huang, H., Using biochar for remediation of soils contaminated with heavy metals and organic pollutants. *Environ. Sci. Pollut. Res.* **2013**, *20*, (12), 8472-8483.
- (38) Uchimiya, M.; Bannon, D. I.; Wartelle, L. H.; Lima, I. M.; Klasson, K. T., Lead retention by broiler litter biochars in small arms range soil: impact of pyrolysis temperature. *J. Agric. Food Chem.* **2012**, *60*, (20), 5035-5044.
- (39) A Vegetation Map of Valles Caldera National Preserve, New Mexico; Highlights of 06-GTR-302; Natural Heritage: Albuquerque, New Mexico, 2006;  
<https://nhnm.unm.edu/sites/default/files/nonsensitive/publications/nhnm/U06MUL01NMUS.pdf>
- (40) A vegetation survey and preliminary ecological assessment of Valles Caldera National Preserve; Highlights of 03-GTR-272; Natural Heritage: Albuquerque, New Mexico, 2003;  
[https://www.fs.usda.gov/Internet/FSE\\_DOCUMENTS/stelprdb5384299.pdf](https://www.fs.usda.gov/Internet/FSE_DOCUMENTS/stelprdb5384299.pdf)
- (41) An Investigation into the Potential Impacts of Watershed Restoration and Wildfire on Water Yields and Water Supply Resilience in the Rio Grande Water Fund Project Area; District, Middle Rio Grande Conservancy, 2017;  
[http://riograndewaterfund.org/wp-content/uploads/2017/01/rgwf\\_stone\\_etal\\_2017.pdf](http://riograndewaterfund.org/wp-content/uploads/2017/01/rgwf_stone_etal_2017.pdf)

- (42) Federation, W. E.; Association, A. P. H., Standard methods for the examination of water and wastewater. *American Public Health Association (APHA): Washington, DC, USA* **2005**.
- (43) Quality of storm water runoff at Los Alamos National Laboratory in 2000 with emphasis on the impact of the Cerro Grande Fire; Highlights of *LA-13926; Los Alamos National Laboratory*, <http://permalink.lanl.gov/object/tr?what=info:lanl-repo/lareport/LA-14177>
- (44) R Core Team *R: A language and environment for statistical computing*; R foundation for statistical computing: Vienna, Austria 2015.
- (45) Seifert, E., OriginPro 9.1: Scientific Data Analysis and Graphing Software-*Software Review. J. Chem. Inf. Model.* **2014**, 54, (5), 1552-1552.
- (46) *Water Quality Survey Summary for the Valles Caldera National Preserve Watershed*; Surface Water Quality Bureau, New Mexico Environment Department; Santa Fe, New Mexico, 2006; <https://www.env.nm.gov/swqb/Surveys/VallesCalderaWQS2001.pdf>
- (47) USEPA STORET Database, <https://www.waterqualitydata.us/portal/31EFkJem020.7> (accessed on Dec 22, 2017)
- (48) Burt, R.; Wilson, M.; Mays, M.; Lee, C., Major and trace elements of selected pedons in the USA. *J. Environ. Qual.* **2003**, 32, (6), 2109-2121.
- (49) Plant tissue analysis and interpretation for vegetable crops in Florida; Highlights of HS964; IFAS Extension, University of Florida, 2003; <http://edis.ifas.ufl.edu/pdffiles/EP/EP08100.pdf>
- (50) Reimann, C.; Ottesen, R. T.; Andersson, M.; Arnoldussen, A.; Koller, F.; Englmaier, P., Element levels in birch and spruce wood ashes—green energy? *Sci. Total Environ.* **2008**, 393, (2), 191-197.
- (51) Etiegni, L.; Campbell, A., Physical and chemical characteristics of wood ash. *Bioresour. Technol.* **1991**, 37, (2), 173-178.
- (52) Tsai, K.-P.; Uzun, H.; Karanfil, T.; Chow, A. T., Dynamic Changes of Disinfection Byproduct Precursors following Exposures of *Microcystis aeruginosa* to Wildfire Ash Solutions. *Environ. Sci. Technol.* **2017**, 51, (15), 8272-8282.
- (53) Gabet, E. J.; Bookter, A., Physical, chemical and hydrological properties of Ponderosa pine ash. *Int. J. Wildland Fire* **2011**, 20, (3), 443-452.
- (54) Wang, J.-J.; Dahlgren, R. A.; Chow, A. T., Controlled burning of forest detritus altering spectroscopic characteristics and chlorine reactivity of dissolved organic matter: effects of temperature and oxygen availability. *Environ. Sci. Technol.* **2015**, 49, (24), 14019-14027.
- (55) de Mendonça, F. G.; da Cunha, I. T.; Soares, R. R.; Tristão, J. C.; Lago, R. M., Tuning the surface properties of biochar by thermal treatment. *Bioresour. Technol.* **2017**, (246), 28-33.
- (56) Fang, Q.; Chen, B.; Lin, Y.; Guan, Y., Aromatic and hydrophobic surfaces of wood-derived biochar enhance perchlorate adsorption via hydrogen bonding to oxygen-containing organic groups. *Environ. Sci. Technol.* **2013**, 48, (1), 279-288.

- (57) Burton, C. A.; Hoefen, T. M.; Plumlee, G. S.; Baumberger, K. L.; Backlin, A. R.; Gallegos, E.; Fisher, R. N., Trace Elements in Stormflow, Ash, and Burned Soil following the 2009 Station Fire in Southern California. *PLoS One*. **2016**, *11*, (5), e0153372.
- (58) Burke, M.; Hogue, T.; Kinoshita, A.; Barco, J.; Wessel, C.; Stein, E., Pre-and post-fire pollutant loads in an urban fringe watershed in Southern California. *Environ. Monit. Assess.* **2013**, *185*, (12), 10131-10145.
- (59) Stein, E. D.; Brown, J. S.; Hogue, T. S.; Burke, M. P.; Kinoshita, A., Stormwater contaminant loading following southern California wildfires. *Environ. Toxicol. Chem.* **2012**, *31*, (11), 2625-2638.
- (60) Alam, M. S.; Swaren, L.; von Gunten, K.; Cossio, M.; Bishop, B.; Robbins, L. J.; Hou, D.; Flynn, S. L.; Ok, Y. S.; Konhauser, K. O., Application of surface complexation modeling to trace metals uptake by biochar-amended agricultural soils. *Appl. Geochem.* **2017**, (in press), 1-10.
- (61) Mohan, D.; Pittman, C. U., Arsenic removal from water/wastewater using adsorbents—a critical review. *J. Hazard. Mater.* **2007**, *142*, (1), 1-53.
- (62) Bhattacharya, A.; Naiya, T.; Mandal, S.; Das, S., Adsorption, kinetics and equilibrium studies on removal of Cr (VI) from aqueous solutions using different low-cost adsorbents. *Chem. Eng. J.* **2008**, *137*, (3), 529-541.
- (63) Kotaš, J.; Stasicka, Z., Chromium occurrence in the environment and methods of its speciation. *Environ. Pollut.* **2000**, *107*, (3), 263-283.
- (64) Bauer, P.; Elbaum, R.; Weiss, I. M., Calcium and silicon mineralization in land plants: transport, structure and function. *Plant Sci.* **2011**, *180*, (6), 746-756.
- (65) Franceschi, V. R.; Nakata, P. A., Calcium oxalate in plants: formation and function. *Annu. Rev. Plant Biol.* **2005**, *56*, 41-71.
- (66) Bogusz, A.; Oleszczuk, P.; Dobrowolski, R., Application of laboratory prepared and commercially available biochars to adsorption of cadmium, copper and zinc ions from water. *Bioresour. Technol.* **2015**, *196*, 540-549.
- (67) Harvey, O. R.; Herbert, B. E.; Rhue, R. D.; Kuo, L.-J., Metal interactions at the biochar-water interface: energetics and structure-sorption relationships elucidated by flow adsorption microcalorimetry. *Environ. Sci. Technol.* **2011**, *45*, (13), 5550-5556.
- (68) Myers-Pigg, A. N.; Louchouart, P.; Amon, R. M.; Prokushkin, A.; Pierce, K.; Rubtsov, A., Labile pyrogenic dissolved organic carbon in major Siberian Arctic rivers: Implications for wildfire-stream metabolic linkages. *Geophys. Res. Lett.* **2015**, *42*, (2), 377-385.
- (69) Lima, I. M.; Boateng, A. A.; Klasson, K. T., Physicochemical and adsorptive properties of fast-pyrolysis bio-chars and their steam activated counterparts. *J. Chem. Technol. Biotechnol.* **2010**, *85*, (11), 1515-1521.
- (70) Cadol, D.; Galanter, A.; Nicholls, P. (2015), Distribution and Transport of Pyrogenic Black Carbon in Soils Affected by Wildfires, Valles Caldera, New Mexico, with Implications for Contaminant

Transport. WRRRI Technical Completion Report No. 365. New Mexico Water Resources Research Institute, Las Cruces, NM.

- (71) Nicholls, P. (2016), Sorption characterization of environmentally relevant concentrations of arsenic and chromium to soils containing pyrogenic black carbon in watersheds affected by wildfires. Unpublished Thesis. New Mexico Institute of Mining and Technology, Socorro, NM.
- (72) Rahman, A.; El Hayek, E.; Blake, J.M.; Bixby, R.; Ali, A.S.; Spilde, M.; Otieno, A; Miltenberger, K.; Ridgeway, C.; Artyushkova, K.; Atudorei, V.; and Cerrato, J.M., *Environ. Sci. Technol.* **2018**, 52, (15), 8115-8123.

## APPENDICES

**APPENDIX A.** Acid extractable elemental content (mg kg<sup>-1</sup>) for wood samples (Pine, Spruce, Aspen) at 60°C, 350°C and 550°C. Data are presented as Mean + standard deviation.

<b>Acid Extractable Elemental Content (mg kg<sup>-1</sup>)</b>												
<b>Temperature: 550°C</b>												
<b>Sample</b>	<b>Al</b>	<b>Ca</b>	<b>Cr</b>	<b>Cu</b>	<b>Fe</b>	<b>K</b>	<b>Mg</b>	<b>Mn</b>	<b>Ni</b>	<b>Si</b>	<b>Sr</b>	<b>Zn</b>
<b>Pine</b>	4138.40	181967.73	476.16	2765.07	5050.52	78075.67	27881.15	1575.62	803.60	814.26	505.93	938.27
	±	±	±	±	±	±	±	±	±	±	±	±
	100.17	6195.55	9.12	302.26	767.95	1781.05	35.82	14.15	22.81	93.11	1.75	4.94
<b>Spruce</b>	4734.25	164204.50	81.50	71.88	4154.38	33847.64	9807.35	3933.69	242.56	334.93	551.96	590.30
	±	±	±	±	±	±	±	±	±	±	±	±
	64.55	3723.07	1.07	1.59	40.74	628.85	106.4	41.92	2.91	29.36	6.25	7.67
<b>Aspen</b>	177.41	307080.02	12.91	72.42	238.57	47800.02	14193.24	175.14	277.82	289.68	1372.46	1209.62
	±	±	±	±	±	±	±	±	±	±	±	±
	3.19	4896.33	2.01	1.62	14.5	728.85	129.61	0.74	1.64	1.58	15.07	12.29
<b>Temperature: 350°C</b>												
<b>Pine</b>	2384.54	122157.57	543.31	4996.51	4151.65	55823.72	19205.62	1179.05	524.65	310.14	332.28	638.32
	±	±	±	±	±	±	±	±	±	±	±	±
	96.48	4502.43	123.69	261.96	441.79	2122.64	747.69	61.36	101.22	18.17	12.89	23.33
<b>Spruce</b>	4477.69	186287.82	112.24	81.47	3598.13	37261.72	6168.71	4760.57	266.93	322.53	646.79	799.14
	±	±	±	±	±	±	±	±	±	±	±	±
	175.93	5459.71	3.06	5.42	908.11	1050.50	48.12	315.24	3.04	23.09	27.32	36.21
<b>Aspen</b>	184.81	294197.49	11.83	62.89	225.13	45153.30	13275.79	182.36	264.34	241.02	1390.40	1206.46
	±	±	±	±	±	±	±	±	±	±	±	±
	1.67	1343.51	0.13	0.60	4.72	242.64	73.52	1.08	3.52	5.76	3.89	8.47
<b>Temperature: 60°C</b>												
<b>Pine</b>	91.1	9364.2	4.97	58.2	114.7	8696.5	466.3	59.6	6.1	202.8	13.1	23.3
	±	±	±	±	±	±	±	±	±	±	±	±
	3.05	220.03	1.29	18.24	45.69	35.69	8.47	2.81	0.25	11.56	0.61	1.81
<b>Spruce</b>	131.5	11294.7	12.9	4.6	198.9	8628.5	419.1	185.1	12.5	258.8	24.3	33.2
	±	±	±	±	±	±	±	±	±	±	±	±
	3.32	248.46	0.46	0.31	7.93	28.68	15.13	6.5	0.9	1.67	0.61	0.4
<b>Aspen</b>	22.2	22359.3	5.1	5.7	22.4	9709.04	858.5	10.6	17.9	23.7	86.8	78.6
	±	±	±	±	±	±	±	±	±	±	±	±
	1.15	565.51	0.03	0.88	8.53	25.86	4.22	0.15	0.82	3.9	0.35	1.49

**APPENDIX B.** The Kruskal Wallis test was used to determine if significant differences exist (defined as p-value < 0.05) among the tree species (Pine, Spruce, Aspen) at three temperatures (60°C, 350°C and 550°C) with respect to acid-extractable metal concentrations (log<sub>10</sub> transformed). Individual contribution of the metals was not considered here due to the limited number of observations (n=3) for each metal. No significant difference (highlighted, p-value =0.4007 > 0.05) were observed for Pine, Aspen and Spruce at 60°C. The limitation of the Kruskal Wallis test is that it does not specify which specific sample is contributing to the overall difference. To address this, the Mann Whitney U test was done to do pairwise comparisons among the samples

Comparison among Pine, Spruce and Aspen at 60°C, 350°C and 550°C (n=9)

<u>Data</u>	<u>χ<sup>2</sup> statistic</u>	<u>p-value</u>
acid extractable element concentrations (log <sub>10</sub> transformed)	89.85	4.982 × 10 <sup>-4</sup>

Comparison among Pine 60, Spruce 60 and Aspen 60 (n=3)

<u>Data</u>	<u>χ<sup>2</sup> statistic</u>	<u>p-value</u>
acid extractable element concentrations (log <sub>10</sub> transformed)	1.8293	0.4007

Comparison among Pine 350, Spruce 350 and Aspen 350 (n=3)


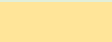
<u>Data</u>	<u>χ<sup>2</sup> statistic</u>	<u>p-value</u>
acid extractable element concentrations (log <sub>10</sub> transformed)	8.1227	0.01723

Comparison among Pine 550, Spruce 550 and Aspen 550 (n=3)

<u>Data</u>	<u>χ<sup>2</sup> statistic</u>	<u>p-value</u>
acid extractable element concentrations (log <sub>10</sub> transformed)	9.5225	0.00855

**APPENDIX C.** The Wilcoxon rank sum test (Mann-Whitney U test) was used to do pairwise comparisons ( $n=9$  samples,  ${}^9C_2=36$  combinations of pairs) of tree species (Pine, Spruce, Aspen) at 60°C, 350°C and 550°C to test for significant differences (defined as  $p < 0.05$ ) in metal concentrations ( $\log_{10}$  transformed). The individual contribution of the metals was not considered here due to the limited number of observations ( $n=3$ ) for each metal.

Serial No.	Pair considered	Diff.	W	<i>p</i> -value	Serial No.	Pair considered	Diff.	W	<i>p</i> -value
1	Aspen 350 – Aspen 60	1.078	990	$1.20 \times 10^{-4}$	19	Pine 60 – Aspen 60	0.164	726	0.383
2	Aspen 550 – Aspen 60	1.108	991	$1.15 \times 10^{-4}$	20	Spruce 60 – Aspen 60	0.331	765	0.190
3	Spruce 550 – Aspen 60	1.407	1043	$8.87 \times 10^{-6}$	21	Spruce 60 – Pine 60	0.642	690	0.103
4	Spruce 350 – Aspen 60	1.477	1053	$5.22 \times 10^{-6}$	22	Aspen 550 – Aspen 350	0.021	672	0.793
5	Pine 350 – Aspen 60	1.678	1080	$1.18 \times 10^{-6}$	23	Spruce 550 – Aspen 350	0.401	788	0.117
6	Pine 550 – Aspen 60	1.748	1101	$3.47 \times 10^{-7}$	24	Spruce 350 – Aspen 350	0.462	798	0.092
7	Aspen 350 – Pine 60	0.761	960	$3.38 \times 10^{-4}$	25	Pine 350 – Aspen 350	0.532	912	$2.64 \times 10^{-3}$
8	Aspen 550 – Pine 60	0.780	967	$2.43 \times 10^{-4}$	26	Pine 550 – Aspen 350	0.634	927	$1.45 \times 10^{-4}$
9	Spruce 550 – Pine 60	1.261	1043	$3.67 \times 10^{-6}$	27	Spruce 550 – Aspen 550	0.371	775	0.155
10	Spruce 350 – Pine 60	1.284	1042	$3.91 \times 10^{-6}$	28	Spruce 350 – Aspen 550	0.434	783	0.130
11	Pine 350 – Pine 60	1.413	1110	$3.06 \times 10^{-8}$	29	Pine 350 – Aspen 550	0.542	911	$2.75 \times 10^{-3}$
12	Pine 550 – Pine 60	1.547	1133	$4.36 \times 10^{-9}$	30	Pine 550 – Aspen 550	0.651	927	$1.45 \times 10^{-3}$
13	Aspen 350 – Spruce 60	0.774	903	$3.73 \times 10^{-3}$	31	Spruce 350 – Spruce 550	0.043	694	0.610
14	Aspen 550 – Spruce 60	0.777	910	$2.86 \times 10^{-3}$	32	Pine 350 – Spruce 550	0.140	738	0.316
15	Spruce 550 – Spruce 60	1.238	1008	$2.91 \times 10^{-5}$	33	Pine 550 – Spruce 550	0.324	783	0.130
16	Spruce 350 – Spruce 60	1.235	1008	$2.91 \times 10^{-5}$	34	Pine 350 – Spruce 350	0.150	713	0.470
17	Pine 350 – Spruce 60	1.339	1114	$2.21 \times 10^{-8}$	35	Pine 550 – Spruce 350	0.282	761	0.207
18	Pine 550 – Spruce 60	1.431	1134	$3.99 \times 10^{-9}$	36	Pine 550 – Pine 350	0.150	738	0.316

 = *p*-value < 0.05 = Significant difference  
 = *p*-value > 0.05 = No significant difference



**APPENDIX D.** BET surface areas (m<sup>2</sup>/g) of the Pine ash samples

Sample	BET surface Area (m <sup>2</sup> /g)
Pine Ash 350°C	36.91
Pine Ash 550°C	294.37

*BET = Brunauer-Emmett-Teller-N<sub>2</sub> surface area*

**APPENDIX E.** Atomic content for the unreacted and reacted 350°C pine ash as determined by X-ray photoelectron spectroscopy (XPS) survey scan.

Sample	% Atomic Content		
	C 1s	O 1s	Cu 2p
Unreacted 350°C pine ash	66.2	33.8	BDL <sup>1</sup>
Reacted 350°C pine ash	73.2	26.7	0.11

<sup>1</sup>*Below detection limit*

**APPENDIX F.** Maximum Contaminant Level (MCL) and different standards for exposure limits set by USEPA for Cr, Cu, Fe, Mn, and Zn. Additionally, average concentrations of these 5 metals in natural soils (without known anthropogenic additions) are also provided for comparison with soil samples collected along the East Fork Jemez river ranges for this study.

Element	Drinking water standard- Maximum Contaminant Level (MCL) ( $\mu\text{g L}^{-1}$ ) <sup>2</sup>	Drinking water action level ( $\mu\text{g L}^{-1}$ ) <sup>3</sup>	Drinking water secondary standard ( $\mu\text{g L}^{-1}$ ) <sup>1</sup>	Surface water human health for the consumption of water + organism ( $\mu\text{g L}^{-1}$ ) <sup>3</sup>	Aquatic Life Freshwater CMC Acute Exposure ( $\mu\text{g L}^{-1}$ )	Aquatic Life Freshwater CCC Chronic Exposure ( $\mu\text{g L}^{-1}$ )	Average concentrations of metals in non-anthropogenically affected soils in the US ( $\text{mg kg}^{-1}$ ) by Burt et al. <sup>5</sup>
Chromium (III)					570	74	
Chromium (total)	100						88.7
Chromium (VI)					16	11	
Copper (Cu)		1300		1300	2 <sup>4</sup>	1.3 <sup>4</sup>	24.7
Iron (Fe)			300			1000	19000
Manganese (Mn)			50	50			62.6
Zinc (Zn)			5000	7400	120	120	589

## References

- (1) USEPA, Secondary Drinking Water Standards: Guidance for Nuisance Chemicals, accessed on Dec 22, 2017 at <https://www.epa.gov/dwstandardsregulations/secondary-drinking-water-standards-guidance-nuisance-chemicals>
- (2) USEPA, National Primary Drinking Water Regulations, accessed on Dec 22, 2017 at <https://www.epa.gov/ground-water-and-drinking-water/table-regulated-drinking-water-contaminants>
- (3) USEPA, National Recommended Water Quality Criteria - Human Health Criteria Table, accessed on Dec 22, 2017 at <https://www.epa.gov/wqc/national-recommended-water-quality-criteria-human-health-criteria-table>
- (4) USEPA, Fact Sheet: Draft Estuarine/Marine Copper Aquatic Life Ambient Water Quality Criteria, accessed on Dec 22, 2017 at <https://www.epa.gov/sites/production/files/2016-08/documents/copper-estuarine-marine-draft-factsheet.pdf>
- (5) Burt, R.; Wilson, M.; Mays, M.; Lee, C., Major and trace elements of selected pedons in the USA. J. Environ. Qual. 2003, 32, (6), 2109-2121.

**APPENDIX G.** Detection limits for analyses using: **a)** inductively coupled plasma optical emission spectrometry (ICP-OES), and **b)** inductively coupled plasma mass spectrometry (ICP-MS).

**a) ICP-OES**

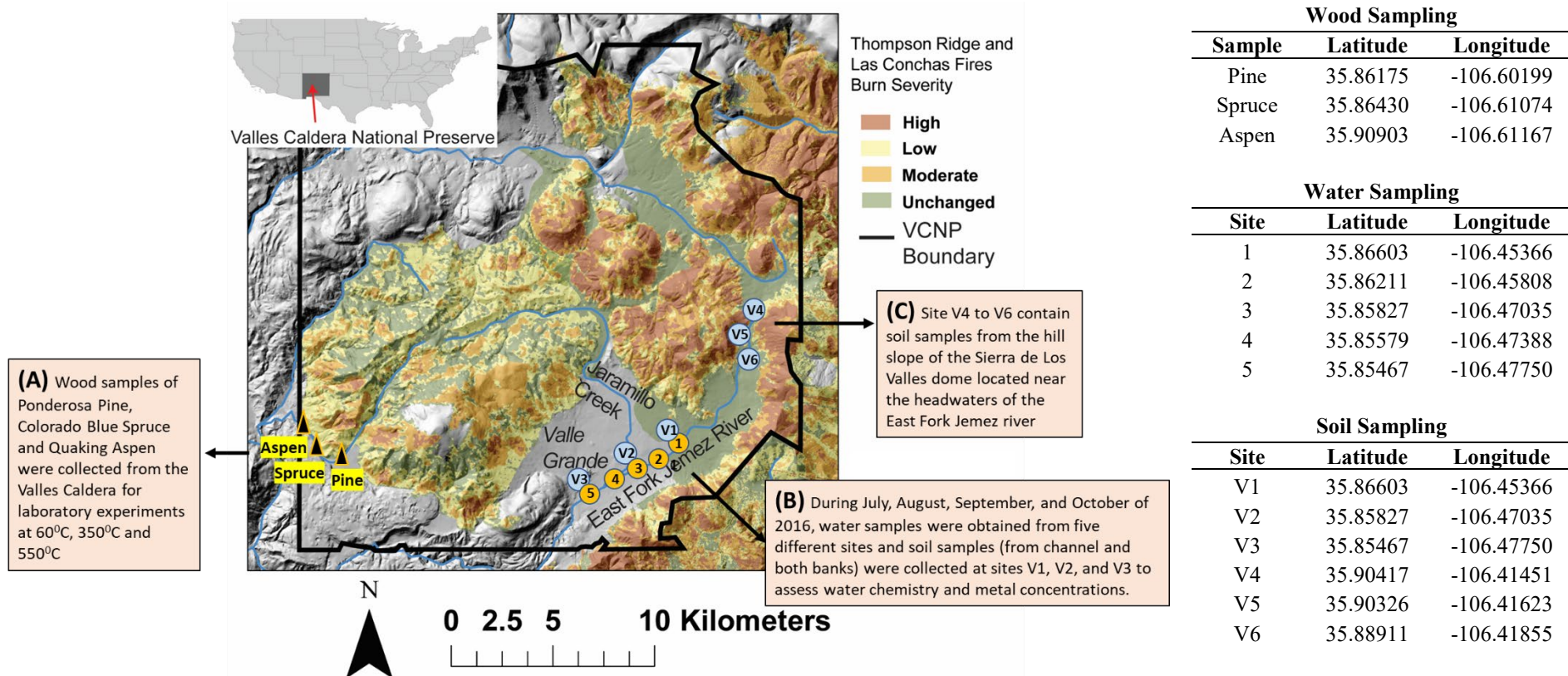
<b>Element</b>	<b>IDL (mg L<sup>-1</sup>)</b>	<b>MDL (mg L<sup>-1</sup>)</b>
Al	0.0280	0.0280
Ca	0.0100	0.0100
Cu	0.0054	0.0054
Fe	0.0062	0.0062
Mg	0.0030	0.0030
Mn	0.0014	0.0014
Ni	0.0150	0.0150
Pb	0.0420	0.0420
V	0.0064	0.0064
Zn	0.0018	0.0018

**b) ICP-MS**

<b>Element</b>	<b>IDL (mg L<sup>-1</sup>)</b>	<b>MDL (mg L<sup>-1</sup>)</b>
Cu	0.004	0.009
Ni	0.006	0.02
Pb	0.0003	0.0004
V	0.006	0.01
Zn	0.04	0.1

\*\*IDL = Instrument Detection Limit

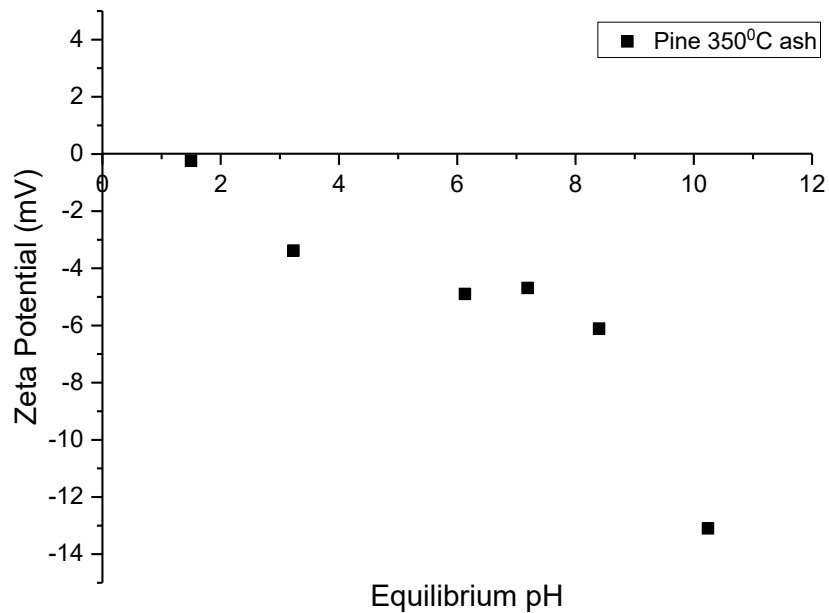
\*\*MDL = Method Detection Limit



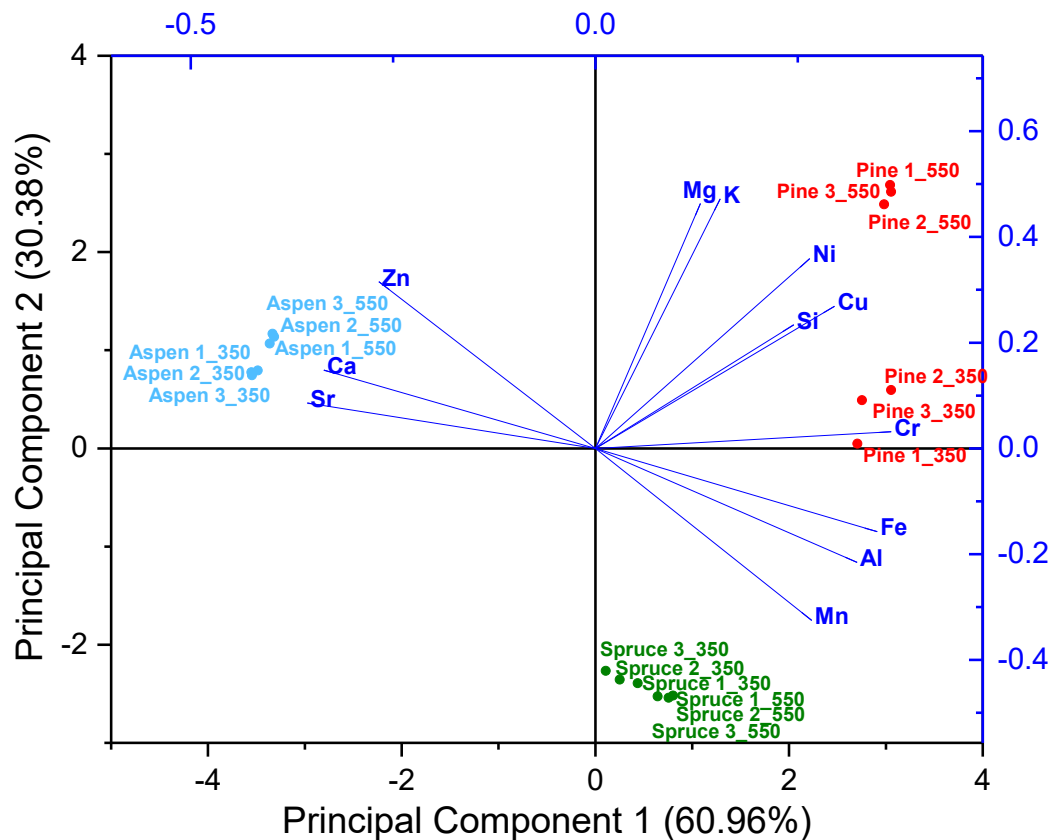
**APPENDIX H.** Map showing the sampling locations for (A) wood, (B) water and soil and (C) soil samples in Valles Caldera. The co-ordinates of the sampling locations are shown beside the map. This site map is adapted from the map published in a previous study by Cerrato et al.<sup>12</sup>

### Reference

- (1) Cerrato, J. M.; Blake, J. M.; Hirani, C.; Clark, A. L.; Ali, A.-M. S.; Artyushkova, K.; Peterson, E.; Bixby, R. J., Wildfires and water chemistry: effect of metals associated with wood ash. *Environ. Sci. Process. Impacts.* **2016**, *18*, (8), 1078-1089.

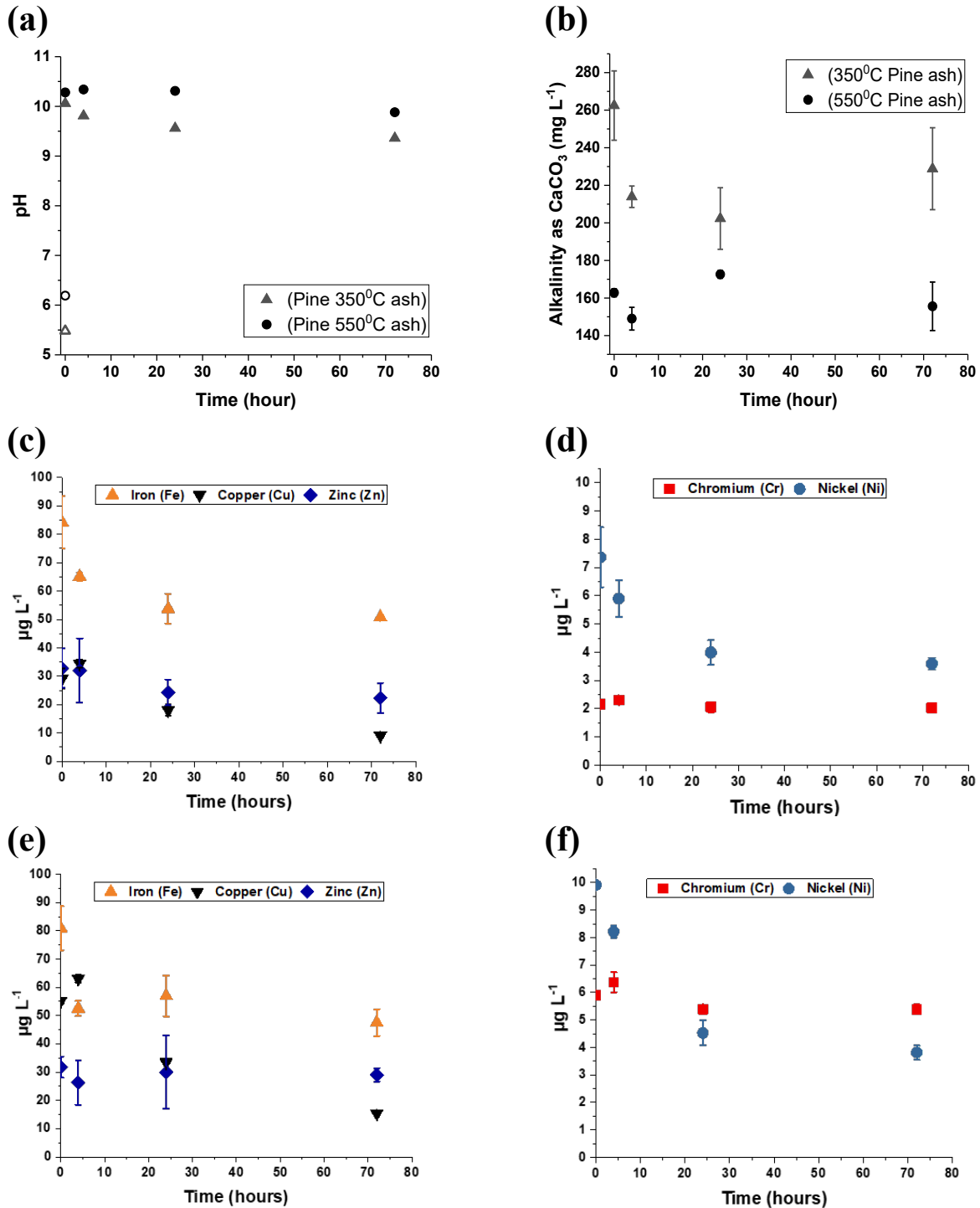


**APPENDIX I.** Zeta Potential (mV) measurements of the Pine 350°C ash in different solution pH values. A Malvern Zetasizer Nano-ZS equipped with a He-Ne laser (633nm) and non-invasive backscatter optics (NIBS) was used for the measurement. The reported values are the average of three independent samples.



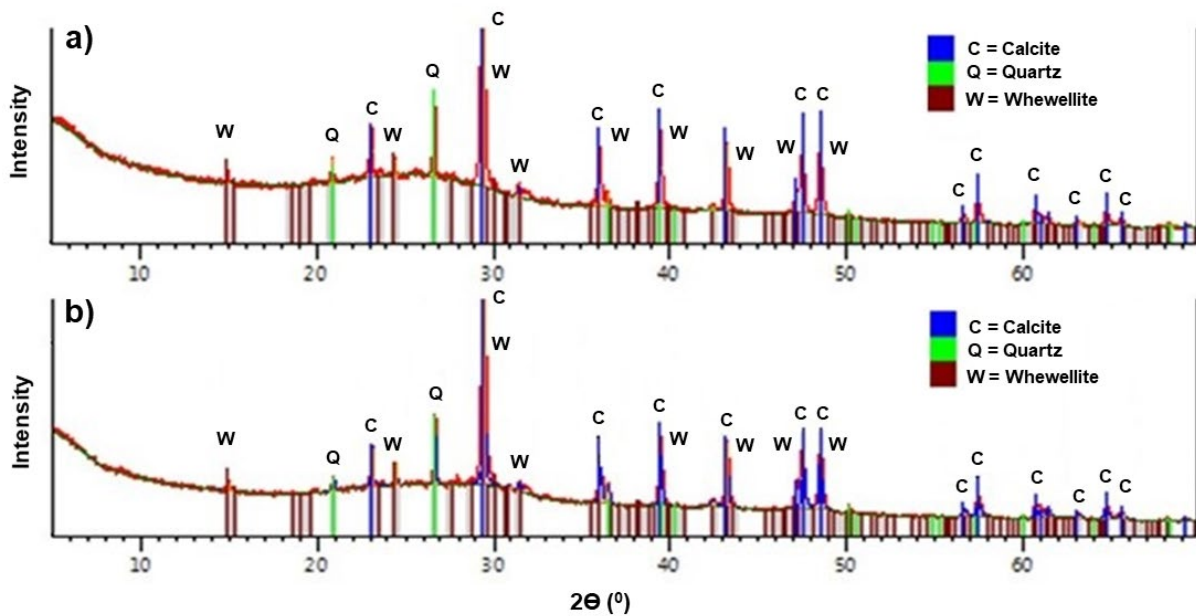
	Coefficients of PC 1	Coefficients of PC 2
Al	<b>0.32329</b>	-0.2157
Ca	-0.33562	<b>0.14808</b>
Cr	<b>0.36557</b>	0.03147
Cu	<b>0.29553</b>	0.26884
Fe	<b>0.34826</b>	-0.15737
K	0.15423	<b>0.47189</b>
Mg	0.12975	<b>0.46318</b>
Mn	<b>0.26729</b>	-0.32558
Ni	0.26484	<b>0.35895</b>
Si	<b>0.24515</b>	0.2337
Sr	-0.35604	<b>0.08592</b>
Zn	-0.26742	<b>0.31536</b>

**APPENDIX J.** Principal component analysis was run on metal concentrations for 350°C and 550°C triplicate measurements of ash samples (Pine, Spruce, Aspen). The first two principal components explained 91.34% of the total variance. The metals such as Al, Cr, Cu, Fe, Mn, and Si showed high positive loadings on PC 1; and PC 2 showed high positive loadings for the major elements (Ca, K, Mg) and metals such as Ni, Sr, and Zn. Coefficients of the metals for the principal components are shown in the table. The figure also shows the component scores of the Pine, Spruce and Aspen ash samples. 350°C and 550°C Pine ash samples had positive scores on the both the principal components.



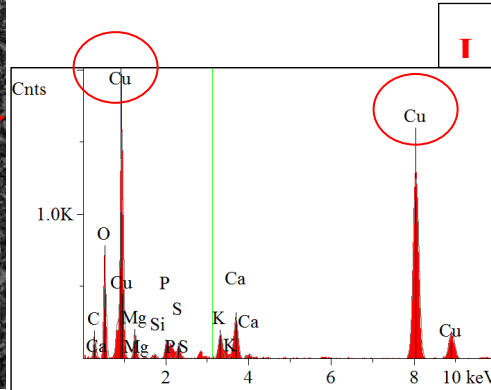
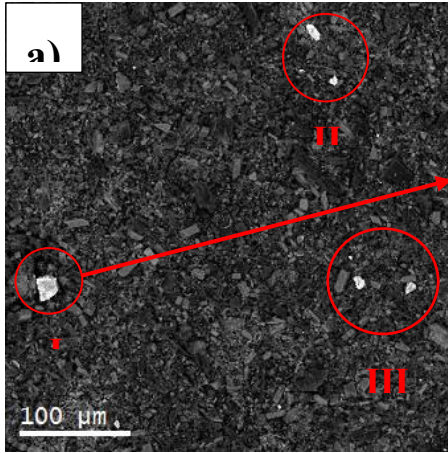
**APPENDIX K.** Concentrations of (c) Fe, Cu, Zn, and (d) Cr, Ni at 0, 4, 24, and 72 hours in reaction of 550°C Pine ash with 18 MΩ water. In figure (e) and (f), metal concentrations are given for the reaction of 350°C Pine ash with 18 MΩ water. pH and alkalinity measured at 0, 4, 24 and 72 hours are shown in figure (a) and (b), respectively. In figure (a), the open symbols represent the pH of 18MΩ water.



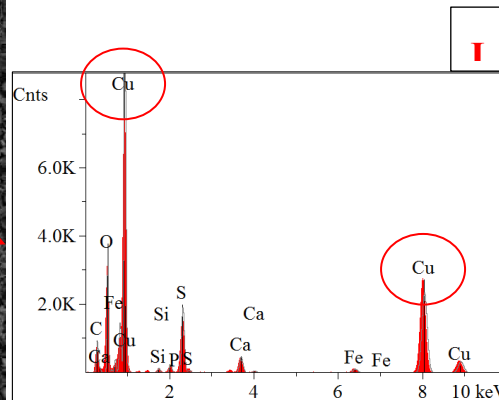
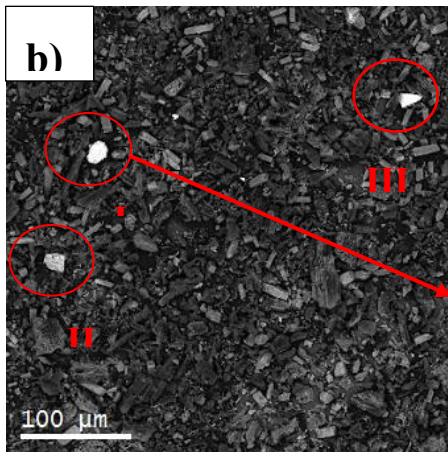


Compound Name	Unreacted Ash (atomic wt.%)	Reacted Ash (atomic wt.%)
Calcite (CaCO <sub>3</sub> )	79%	78%
Quartz (SiO <sub>2</sub> )	12%	11%
Whewellite (Ca(C <sub>2</sub> O <sub>4</sub> ).H <sub>2</sub> O)	9%	11%

**APPENDIX L.** XRD patterns of the (a) reacted and the (b) unreacted 350°C Pine ash sample from the batch sorption experiments with Cu(II). The two samples are very similar in terms of crystalline composition which is predominantly calcite (78-79 %) with lesser amounts of quartz (11-12 %) and whewellite (9-11 %).

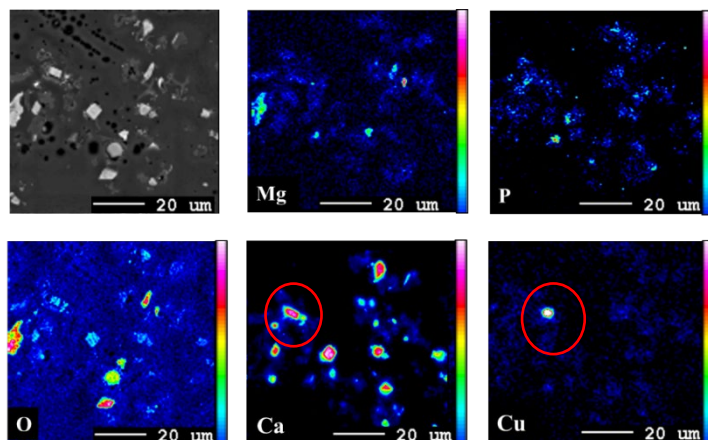
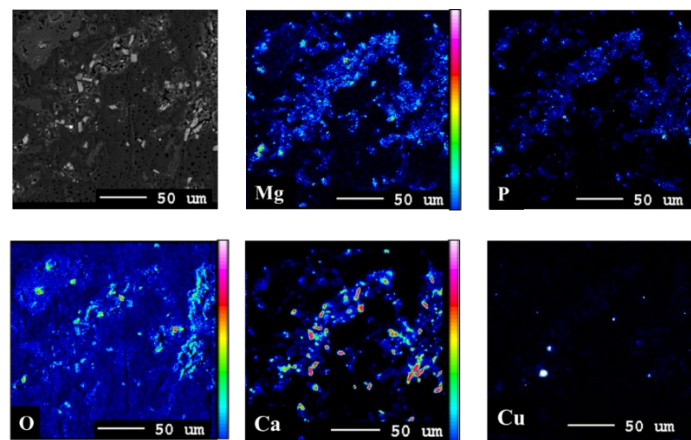
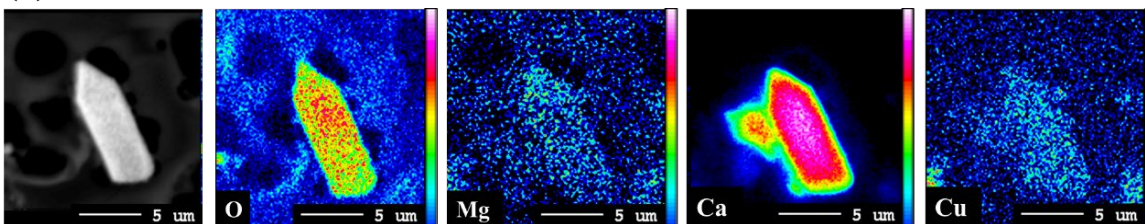


Element	Conc.	Units
C	7.16	wt.%
O	12.60	wt.%
Mg	2.91	wt.%
P	1.34	wt.%
S	0.98	wt.%
Ca	3.09	wt.%
K	1.87	wt.%
Si	0.36	wt.%
Al	0.21	wt.%
Cu	69.51	wt.%
Total	100.0	wt.%



Element	Conc.	Units
C	21.42	wt.%
O	1.33	wt.%
Si	0.59	wt.%
P	0.96	wt.%
S	7.66	wt.%
Ca	3.32	wt.%
Fe	1.17	wt.%
Cu	63.55	wt.%
Total	100.0	wt.%

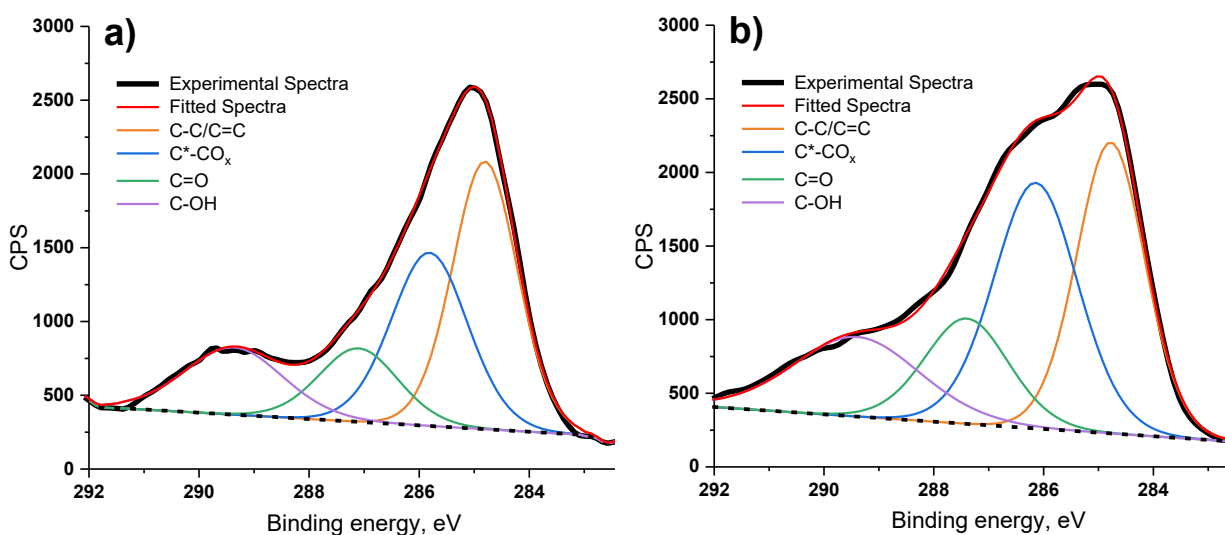
**APPENDIX M.** SEM images of the **(a)** unreacted and the **(b)** reacted 350°C Pine ash from the batch sorption experiments with Cu(II). EDS spectrum from a Cu grain on both the ash samples shows the presence of Cu peaks. The atomic wt.% distribution for the respective spectrum is also shown here.

**(a)****(b)****(c)** Microprobe mapping of the mineralized Ca region [red circled in figure (a)] of the reacted ash**(d)**

	K (wt%)	Ca (wt%)	Mg (wt%)	Cu wt%	Si (wt%)	S (wt%)	P (wt%)	O (wt%)	C (wt%)	Total (wt%)
Average of 7 reference lines (Reacted sample)	0.03	16.96	0.02	0.01	0.01	0.01	0.10	46.43	14.82	78.38
Average of 7 reference lines (Unreacted sample)	0.14	17.56	0.01	BDL*	BDL	0.05	0.01	46.27	14.69	78.73

\*BDL = Below detection limit at 95% confidence interval

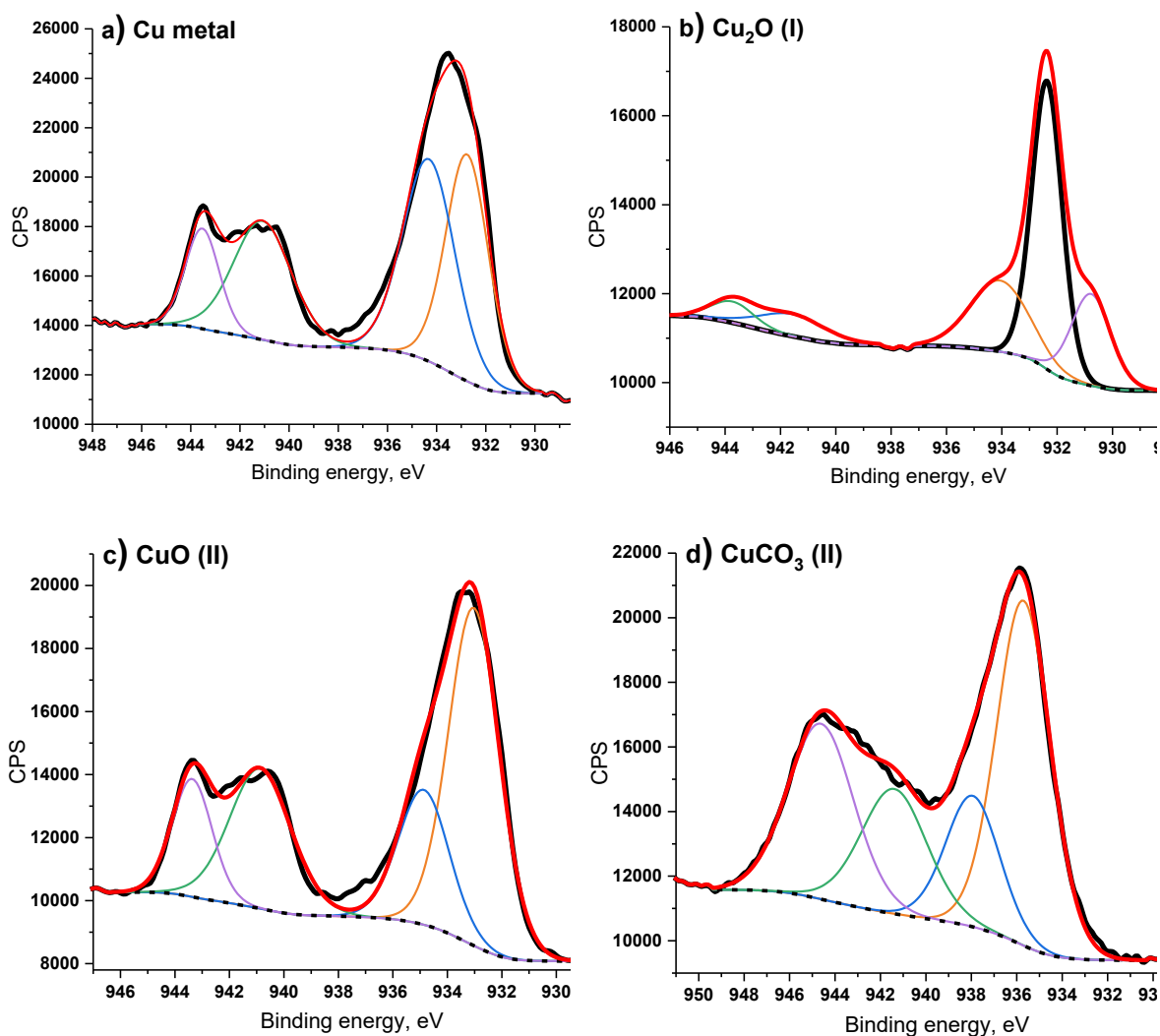
**APPENDIX N.** Microprobe mapping of Mg, P, O, Ca, and Cu on the **(a)** reacted and **(b)** unreacted 350°C Pine ash. Microprobe analysis showed the presence of low levels of detectable Cu associated with mineralized Ca in the reacted ash, shown in figure **(c)**. In table **(d)**, the wt% of the elements associated with the mineralized Ca region is shown. At the 95% confidence level, the Cu in the reacted sample is detectable at 0.012 wt% but is below the detection limit in the unreacted sample. The detection limit for Cu at 95% confidence level was 0.009 wt%.



**(c)** Percentages of surface carbon bonds determined from curve fitting of C 1s high resolution XPS spectra

	C-C %	C*-CO <sub>x</sub> %	C=O %	C-OH %
<b>Binding energy, eV</b>	<b>285</b>	<b>285.6</b>	<b>287.5</b>	<b>289.5</b>
Untreated ash	35.3	16.8	4.7	9.4
Reacted ash	25.3	24.2	11.9	11.8

**APPENDIX O.** XPS high resolution C 1s spectra for the (a) Unreacted 350°C Pine ash sample, and (b) the reacted 350°C Pine ash sample. (c) Percent compositions of the C 1s spectra for the unreacted and the reacted ash.



**(e)** Binding energy values obtained for reference samples using XPS high resolution Cu 2p spectra

Reference Samples	Binding Energy (eV)
Cu metal	932.8
Cu <sub>2</sub> O (I)	932.4
CuO (II)	934.9
CuCO <sub>3</sub> (III)	935.7

**APPENDIX P.** XPS high-resolution Cu 2p spectra for **(a)** Cu metal, **(b)** Cu<sub>2</sub>O (I), **(c)** CuO (II) and **(d)** CuCO<sub>3</sub> (II). **(e)** The binding energies obtained for the Cu 2p regions for these reference materials are shown.